JOINT EUROPEAN TORUS JET

JET–P(89)13

T.P. Hughes, S.R.P. Smith
and JET Team

Effects of Plasma Dielectric Properties on Thomson Scattering of Millimetre Waves in Tokamak Plasmas

Effects of Plasma Dielectric Properties on Thomson Scattering of Millimetre Waves in Tokamak Plasmas

T.P. Hughes, S.R.P. Smith[1]
and JET Team*

JET-Joint Undertaking, Culham Science Centre, OX14 3DB, Abingdon, UK

Department of Physics, University of Essex, Wivenhoe Park, Colchester CO4 3SQ, U.K.
** See Appendix 1*

Preprint of Paper to be submitted for publication in
Journal of Plasma Physics

ABSTRACT

Thomson scattering from a magnetized plasma is considered, taking into account the dielectric properties of the plasma. General results for the geometrical form factor are given in explicit form. The scattered power detectable by a heterodyne receiver is discussed and some numerical calculations are presented. The results are applied to the scattering of millimetre waves in tokamak plasmas near the electron plasma and electron cyclotron frequencies.

1. INTRODUCTION

Millimetre wave Thomson scattering observations have been proposed as a diagnostic technique for studying particle velocity distribution functions in tokamak plasmas (Woskoboinikow et al. 1983). In a detailed study of this technique it is regrettably necessary to discard a number of the simplifying assumptions commonly made in discussing conventional scattering at much shorter (visible or infrared) wavelengths. The scattering cross-section must be recalculated taking into account the effects of the dielectric properties of the plasma, and the propagation of the incident and scattered radiation must be carefully considered.

Bretz (1987) has discussed geometrical effects on the scattering cross-section, giving detailed consideration to the specific case of X- to X- mode scattering in the plane perpendicular to the magnetic field. In this paper we consider the general problem for any scattering geometry and for any incident and scattered polarizations. The results are given in Section 4, and in explicit form suitable for numerical calculations in Appendix 1. In Section 5 we find an expression for the scattered power detectable by a heterodyne receiver outside the plasma, and in Section 7 we present some numerical results for the geometrical form factor. The practical application of the results to scattering experiments is considered in Section 8.

A list of symbols is given in Appendix 2.

2. CHARACTERISTIC WAVES

A characteristic wave in a uniform magnetized plasma is an electromagnetic wave which does not change its state of polarization as it propagates. At a given frequency, for given plasma parameters and a specified direction of propagation there are in general two characteristic waves with different polarizations, the O and X modes, though one or both may not be able to propagate.

Consider now a non-uniform plasma with continuous gradients of electron density and magnetic field, into which a wave is launched at the edge as a characteristic wave, i.e. as an O or X mode wave. It has been shown (Hutchinson 1979, Boyd 1985) that in tokamak plasmas, if the wave propagates in the poloidal plane, its polarization will change as it moves through the plasma, but in such a

way that the wave remains in the same mode for the local plasma conditions. It has yet to be verified experimentally that the same behaviour occurs for arbitrary directions of propagation, but this is generally assumed to be a satisfactory approximation and is the basis of ray tracing codes, e.g. TORAY (Kritz et al. 1983). We therefore refer to an O or X mode wave propagating through the non-uniform plasma.

Near the edge of the plasma the electron density is too low and the anisotropy insufficient to modify the polarization so as to maintain a pure characteristic mode. Calculations by Boyd (1988) and by Airoldi et al. (1988) indicate that for JET conditions a few percent of the power launched in a characteristic mode from an antenna at the wall may be converted into the orthogonal polarization on its way into the region of denser plasma. The effect will be neglected in this paper.

When considering the propagation of millimeter waves in tokamak plasmas ($T_e \sim 1$ to 10 keV, $n_e \sim 10^{19}$ to 10^{20} m^{-3}) the cold plasma approximation may safely be used except for calculations of damping, which will not be considered here (Batchelor et al. (1980)). Relativistic effects will be ignored. For a wave of angular frequency ω the appropriate form for the dielectric tensor $\underline{\underline{\epsilon}}$, defined by $\nabla \times (\nabla \times \underline{E}) = (\frac{\omega}{c})^2 \, \underline{\underline{\epsilon}} \cdot \underline{E}$, when the applied magnetic field $\underline{B}$ is in the z direction is (see e.g. Heald and Wharton (1965))

$$\underline{\underline{\epsilon}} = \begin{bmatrix} \epsilon_1 & -i\epsilon_2 & 0 \\ i\epsilon_2 & \epsilon_1 & 0 \\ 0 & 0 & \epsilon_3 \end{bmatrix} . \qquad (1)$$

Here

$$\epsilon_1 = 1 - \frac{\alpha}{1 - \beta}$$

$$\epsilon_2 = \frac{\alpha \, \beta^{1/2}}{1 - \beta}$$

$$\epsilon_3 = 1 - \alpha$$

and

$$\alpha = \omega_{pe}^2/\omega^2 \quad ,$$

$$\beta = \omega_{ce}^2/\omega^2 \quad ,$$

$\omega_{pe} = \left(\frac{n_e e^2}{m_e \epsilon_0} \right)^{1/2}$ being the electron plasma frequency and $\omega_{ce} = \frac{eB}{m_e}$ the electron cyclotron frequency.

For a wave whose wave vector $\underline{k}$ lies in the (x,z) plane at an angle ϕ to the z axis (and $\underline{B}$), the refractive index $\mu(\phi) = \frac{ck}{\omega}$ is found by solving the equation

$$\begin{bmatrix} \mu^2\cos^2\phi - \epsilon_1 & i\epsilon_2 & -\mu^2\cos\phi\sin\phi \\ -i\epsilon_2 & \mu^2 - \epsilon_1 & 0 \\ -\mu^2\cos\phi\sin\phi & 0 & \mu^2\sin^2\phi - \epsilon_3 \end{bmatrix} \begin{bmatrix} E_x \\ E_y \\ E_z \end{bmatrix} = 0 \qquad (2)$$

where E_x, E_y, E_z are components of the complex wave electric field $\underline{E}$, whose real part is to be interpreted as the actual physical field. The result is the Appleton-Hartree equation for a cold plasma: the refractive index μ_λ for a wave of polarization λ is given (Stix (1962), p.39) by

$$\mu_\lambda^2 = 1 - \frac{2\alpha\,(1-\alpha)}{2(1-\alpha) - \beta\sin^2\phi + \lambda\gamma^{1/2}} \qquad (3)$$

where

$$\gamma = (\beta\sin^2\phi)^2 + 4\beta\,(1-\alpha)^2\cos^2\phi$$

and

$$\lambda = +1 \text{ for the O mode}$$
$$\text{or } -1 \text{ for the X mode} \quad .$$

(An expression given by Heald and Wharton (1965) p.23 is valid only for $\alpha \leq 1$). In the special case where $\underline{k} \perp \underline{B}$, i.e. $\phi = \frac{\pi}{2}$, for the O mode

$$\mu_+^2 = 1 - \alpha \qquad (\phi = \pi/2)$$

while for the X mode

$$\mu_-^2 = 1 - \frac{\alpha(1-\alpha)}{1-\alpha-\beta} \qquad (\phi = \pi/2) \quad . \tag{3a}$$

The polarization forms of the two characteristic waves with $\underline{k}$ at angle ϕ to $\underline{B}$ in the (x,z) plane are found from equation (2). From the second row

$$\left(\frac{E_Y}{E_X}\right)_\lambda = \frac{i\epsilon_2}{\mu_\lambda^2 - \epsilon_1}$$

and from the third row

$$\left(\frac{E_Z}{E_X}\right)_\lambda = \frac{\mu_\lambda^2 \cos\phi \sin\phi}{\mu_\lambda^2 \sin^2\phi - \epsilon_3} \quad .$$

Then the <u>un-normalized</u> polarization vector $\underline{e}_\lambda$, defined by $\underline{E}_\lambda = A_\lambda \cdot \underline{e}_\lambda$, where A_λ is a normalizing factor, is

$$\underline{e}_\lambda = \{\, 1, \frac{i\epsilon_2}{\mu_\lambda^2 - \epsilon_1}, \frac{\mu_\lambda^2 \cos\phi \sin\phi}{\mu_\lambda^2 \sin^2\phi - \epsilon_3} \,\} \quad . \tag{4}$$

Expression (4) is not appropriate for the case when $\phi = \pi/2$ because $E_{+Z} \to \infty$. In this case we write

$$\underline{e}_{+\,(\phi = \frac{\pi}{2})} = \{\, 0,0,1 \,\}$$

for the O-mode, and

$$\underline{e}_{-\,(\phi = \frac{\pi}{2})} = \{\, 1, -i\frac{\epsilon_1}{\epsilon_2}, 0 \,\} \tag{4a}$$

for the X-mode (there is a misprint in Bretz (1987) for E_{-y}).

3. ENERGY FLUX AND RAY DIRECTION

In a cold plasma the Poynting vector of a wave gives the electromagnetic energy flux (see e.g. Bekefi 1966):

$$\underline{W} = \tfrac{1}{4} \, (\underline{E} \times \underline{H}^* + \underline{E}^* \times \underline{H}) \quad . \tag{5}$$

The energy travels with the group velocity

$$\underline{v}_{g\lambda} = \left(\frac{\partial \omega}{\partial \underline{k}} \right)_\lambda = \frac{\partial}{\partial \underline{k}} \left(\frac{ck}{\mu_\lambda} \right) . \tag{6}$$

For millimetre waves in tokamak plasmas it is assumed that the refractive index of the plasma varies slowly, i.e. the scale length of the refractive index variations is much longer than the wavelength of the radiation, so the methods of geometrical optics may be used to follow the flux of energy and the variation of the polarization of a characteristic wave along a ray path. The ray travels in the direction of the group velocity.

For a given frequency there are two wave vector surfaces defined by $\underline{k}$, one for each polarization O or X. Each is a surface of revolution about the direction of $\underline{B}$. The normal to the surface for a given direction of $\underline{k}$ defines the direction of the corresponding ray at that point in the plasma.

We consider a magnetized plasma with $\underline{B}$ in the z direction. For a wave of polarization λ with wave vector direction $\hat{\underline{k}}$ in the (x,z) plane at an angle ϕ to z (and $\underline{B}$), the group velocity is given by

$$\underline{v}_{g\lambda} = \frac{c}{\mu_\lambda} \left[\hat{\underline{k}} - \frac{1}{\mu_\lambda} \frac{\partial \mu_\lambda}{\partial \phi} \hat{\underline{p}} \right] \tag{7}$$

where $\hat{\underline{p}} = \{ \cos \phi, \, 0, \, - \sin \phi \}$ is the unit vector normal to $\hat{\underline{k}}$ in the (x,z) plane. The ray direction with unit vector $\hat{\underline{r}}_\lambda$ is therefore also in the (x,z) plane, at an angle say ρ_λ to the z direction:

$$\hat{\underline{r}}_\lambda = \{ \sin \rho_\lambda, \; 0, \; \cos \rho_\lambda \} \; . \qquad (8)$$

The angle δ_λ between the direction of the wave vector and that of the ray (see Figure 1) is given by

$$\delta_\lambda = (\phi - \rho_\lambda) = \tan^{-1} \left(\frac{1}{\mu_\lambda} \frac{d\mu_\lambda}{d\phi} \right)$$

$$= \tan^{-1} \left[\frac{-\lambda(1 - \mu_\lambda^2) \; \beta \cos \phi \sin \phi}{\gamma^{\frac{1}{2}}} \right] \qquad (9)$$

from equation (3).

For O-mode waves a ray direction is associated with a single $\underline{k}$ vector, but for X-mode waves there may be up to three different $\underline{k}$ vectors producing rays in the same direction. In a scattering experiment, therefore, up to three different contributions to X-mode scattering may have the same ray direction in the scattering volume. Fortunately, in an inhomogeneous plasma the paths followed by the rays will separate as they propagate away, and usually only one will reach the detector antenna within the field of view, though in some geometries there may be a problem of "spatial multiplexing".

The shape of the wave vector surface is clearly important when considering the transfer of energy from the geometrical optics viewpoint (Mercier 1964). The Gaussian curvature of the surface is $C_{G\lambda} = \frac{C_\lambda}{k^2}$, where

$$C_\lambda = \left[1 + \sin^2\delta_\lambda - \frac{\cos^2\delta_\lambda}{\mu_\lambda} \frac{d^2\mu_\lambda}{d\phi^2} \right] \frac{\sin \rho_\lambda \cos \delta_\lambda}{\sin \phi} \qquad (10)$$

for polarization λ (Simonich and Yeh 1971). It is related to the curvature S_λ of the refractive index surface:

$$S_\lambda = \frac{\omega^2}{c^2} \; C_{G\lambda} = \frac{C_\lambda}{\mu_\lambda^2} \; . \qquad (11)$$

The "ray refractive index" $\mu_{r\lambda}$ used by Bekefi (1966), which is also known as the "convergence refractive index" (Mercier 1964), is given by

$$\mu_{r\lambda}^2 = \frac{\mu_\lambda^2}{|C_\lambda|} \quad . \tag{12}$$

An explicit expression for C_λ is given in Appendix 1, Section 5.

Provided there is no absorption or emission or scattering when a pencil of radiation passes through a medium, it can be shown (Bekefi (1966), p.33) that

$$\frac{I_\lambda}{\mu_{r\lambda}^2} = \text{constant} \quad , \tag{13}$$

I_λ being the specific intensity in watts m^{-2} per radian frequency interval per steradian of ray solid angle in mode λ. This is a very useful result.

We shall also need to relate the element of <u>ray</u> solid angle $d\Omega_r$ to the element of <u>wave vector</u> solid angle $d\Omega_k$.

Now

$$\left(\frac{d\Omega_r}{d\Omega_k} \right)_\lambda = \frac{\sin \rho_\lambda d\rho_\lambda \, d\psi}{\sin \phi \, d\phi \, d\psi} \tag{14}$$

where ψ is the angle of rotation about the Z axis, and $\rho_\lambda = \phi - \delta_\lambda$, so

$$\frac{d\rho_\lambda}{d\phi} = 1 - \frac{d\delta_\lambda}{d\phi}$$

$$= 1 + \sin^2\delta_\lambda - \frac{\cos^2\delta_\lambda}{\mu_\lambda} \frac{d^2\mu_\lambda}{d\phi^2} \tag{15}$$

from expression (9).

Thus

$$\left(\frac{d\Omega_r}{d\Omega_k}\right)_\lambda = \frac{\sin\rho_\lambda}{\sin\phi}\left[1 + \sin^2\delta_\lambda - \frac{\cos^2\delta_\lambda}{\mu_\lambda}\frac{d^2\mu_\lambda}{d\phi^2}\right]$$

$$= \frac{C_\lambda}{\cos\delta_\lambda} = \frac{\mu_\lambda^2}{\mu_{r\lambda}^2\cos\delta_\lambda} \quad . \tag{16}$$

4. THE DIFFERENTIAL SCATTERING CROSS-SECTION

In this section the differential scattering cross-section will be derived and the results compared with expressions given by other authors.

Consider a plane monochromatic incident wave entering a scattering volume V in a plasma. The electric field of the wave will be written as

$$\underline{E}_{I\lambda}(\underline{r},t) = A_{I\lambda}\cdot\underline{e}_{I\lambda}\ \exp\left[i(\underline{k}_{I\lambda}\cdot\underline{r} - \omega_I t)\right] \tag{17}$$

where $\underline{e}_I$ is the un-normalized polarization vector.

An electron in this field will obey the equation of motion

$$m_e\frac{d\underline{v}}{dt} = -e\left[\underline{E}_{I\lambda} + \underline{v}\times\underline{B}\right] = -i\omega_I m_e\underline{v} \quad . \tag{18}$$

The motion of the electrons represents an induced current, with current density

$$\underline{j}_I = -n_e e\,\underline{v} = \underline{\underline{\sigma}}_I\cdot\underline{E}_{I\lambda} \tag{19}$$

where the conductivity $\underline{\underline{\sigma}}$ is related to the dielectric tensor:

$$\underline{\underline{\sigma}}_I = (\underline{\underline{I}} - \underline{\underline{\epsilon}}_I)\,i\omega_I\epsilon_o \quad . \tag{20}$$

Fluctuations in the electron density produce a fluctuating contribution to the current density of

$$\delta\,\underline{j}_I = -\delta n_e\,e\,\underline{v} = \frac{\delta n_e}{n_e}\ (\underline{\underline{\sigma}}_I\cdot\underline{E}_{I\lambda}) = \underline{j}_S \tag{21}$$

which acts as a source for the scattered field $\underline{E}_S(\underline{r},t)$. We now seek an expression for the scattered power with frequency ω_S and wave number direction $\hat{\underline{k}}_S$.

Define the space-time Fourier transform of an arbitrary function $A(\underline{r},t)$ as

$$\left.\begin{aligned} A^T(\underline{k},\omega) &= \int d^3\underline{r} \int dt\, e^{-i(\underline{k}\cdot\underline{r}-\omega t)}\, A(\underline{r},t) \\ A(\underline{r},t) &= \frac{1}{(2\pi)^4} \int d^3\underline{k} \int d\omega\, e^{i(\underline{k}\cdot r-\omega t)}\, A^T(\underline{k},\omega)\ . \end{aligned}\right] \qquad (22)$$

Formally, the space and time integrals are to be evaluated in the limits of infinite volume V and time τ.

The inhomogeneous equation satisfied by $\underline{E}_S^T(\underline{k}_S,\omega_S)$ is

$$\underline{k}_S \times (\underline{k}_S \times \underline{E}_S^T) - (\omega_S/c)^2\, (\underline{\underline{\epsilon}}_S \cdot \underline{E}_S^T) = -\, i(\omega_S/c^2\epsilon_0)\underline{j}_S^T\ . \qquad (23)$$

The solution of this equation is

$$\underline{E}_S^T = \sum_\nu a_\nu\, \underline{e}_{S\nu}\ , \qquad (24)$$

where the eigenfunctions $\underline{e}_{S\nu}$ satisfy the dispersion relation - the homogeneous eigenvalue equation

$$k_{S\nu}^2\, [\, \underline{e}_{S\nu} - \hat{\underline{k}}_S(\hat{\underline{k}}_S\cdot\underline{e}_{S\nu})\,] - (\omega_S/c)^2\, (\underline{\underline{\epsilon}}_S \cdot \underline{e}_{S\nu}) = 0\ , \qquad (25)$$

with eigenvalues $k_{S\nu}{}^2 = \mu_{S\nu}{}^2(\hat{\underline{k}}_S)\ (\omega_S/c)^2$. In principle, ν takes on three values, but the third value (besides $\nu = \pm 1$) corresponds to longitudinal fields that are not relevant here. Since $\underline{\underline{\epsilon}}_S$ is Hermitian, the orthogonality condition is

$$\underline{e}^*_{S\nu'} \cdot \underline{\underline{\epsilon}}_S \cdot \underline{e}_{S\nu} = \delta_{\nu'\nu}\, (\underline{e}^*_{S\nu} \cdot \underline{\underline{\epsilon}}_S \cdot \underline{e}_{S\nu})\ . \qquad (26)$$

Thus

$$a_\nu = \frac{-ik_{S\nu}^2 \ (\underline{e}_{S\nu}^* \cdot \underline{j}_S^T)}{(k_S^2 - k_{S\nu}^2) \ \epsilon_0 \ \omega_S \ (\underline{e}_{S\nu}^* \cdot \underline{\underline{\epsilon}}_S \cdot \underline{e}_{S\nu})}. \tag{27}$$

The average total scattered power generated inside the scattering volume V is

$$P_S = \frac{1}{4} \int d^3\underline{r} \ \ \overline{(\underline{E}_S \cdot \underline{j}_S^* + \underline{E}_S^* \cdot \underline{j}_S)}$$

$$= -\frac{\tau^{-1}}{4(2\pi)^8} \int d^3\underline{k}_S d^3\underline{k}_S' d\omega_S d\omega_S' \ d^3\underline{r} \int_{-\tau/2}^{\tau/2} dt \ e^{i\{(\underline{k}_S - \underline{k}_S')\cdot\underline{r} - (\omega_S - \omega_S')t\}} \ x$$

$$x \ [\ \underline{E}_S^T \ (\underline{k}_S, \omega_S) \cdot \underline{j}_S^T \ (\underline{k}_S', \omega_S')^* + \underline{E}_S^T (\underline{k}_S', \omega_S')^* \cdot \underline{j}_S^T (\underline{k}_S, \omega_S) \ ]$$

$$= -\frac{\tau^{-1}}{4(2\pi)^4} \int d^3\underline{k}_S \int d\omega_S \ \langle \ \underline{E}_S^T (\underline{k}_S, \omega_S)^* \cdot \underline{j}_S^T \ (\underline{k}_S, \omega_S) + \underline{E}_S^T (\underline{k}_S, \omega_S) \cdot \underline{j}_S^T (\underline{k}_S, \omega_S)^* \ \rangle \tag{28}$$

taken in the limit $\tau \to \infty$. Here $\langle \ldots \rangle$ denotes an ensemble average.

The power emitted per scattered frequency range $d\omega_S$ per solid angle $d\Omega_{kS}$ in wave vector space in the direction $\hat{\underline{k}}_S$, $d^2P_S/d\Omega_{kS}d\omega_S$, is found by replacing the element of volume $d^3\underline{k}_S$ in wave vector space by $k_S^2 dk_S d\Omega_{kS}$. Then

$$\frac{d^2P_S}{d\Omega_{kS}d\omega_S} = -\frac{\tau^{-1}}{4(2\pi)^4} \int k_S^2 \ dk_S \ \langle \underline{E}_S^T \ (\underline{k}_S, \omega_S)^* \cdot \underline{j}_S^T \ (\underline{k}_S, \omega_S)$$

$$+ \underline{E}_S^T (\underline{k}_S, \omega_S) \cdot \underline{j}_S^T \ (\underline{k}_S, \omega_S)^* \rangle$$

$$= -\frac{\tau^{-1}}{4(2\pi)^4} \sum_\nu \int k_{S\nu}^2 dk_{S\nu} \langle a_\nu^* \underline{e}_{S\nu}^* \cdot \underline{j}_S^T + a_\nu \underline{e}_{S\nu} \cdot \underline{j}_S^{T*} \rangle$$

$$= \tau^{-1} \sum_\nu \left\langle \frac{k_{S\nu}^3 \ |\underline{e}_{S\nu}^* \cdot \underline{j}_S^T \ (\underline{k}_{S\nu}, \omega_S)|^2}{64 \ \pi^3 \epsilon_0 \omega_S \ (\underline{e}_{S\nu}^* \cdot \underline{\underline{\epsilon}}_S \cdot \underline{e}_{S\nu})} \right\rangle .$$

Now $\underline{j}_S^T = \dfrac{\delta n_e(\underline{k},\omega)}{n_e}\ (\underline{\underline{\sigma}}_I \cdot \underline{e}_{I\lambda})\ A_{I\lambda}$, so

$$\frac{d^2P_S}{d\Omega_{kS}d\omega_S} = \tau^{-1} \sum_\nu \left\langle \frac{\mu_{S\nu}^3 \omega_S^2\ \omega_I^2\ \epsilon_0\ |A_{I\lambda}|^2\ |\underline{e}_{S\nu}^* \cdot (\underline{\underline{I}}-\underline{\underline{\epsilon}}_I)\cdot\underline{e}_{I\lambda}|^2\ |\delta n_e^T(\underline{k},\omega)|^2}{64\ \pi^3\ c^3\ n_e\ (\underline{e}_{S\nu}^*\cdot\underline{\underline{\epsilon}}_S\cdot\underline{e}_{S\nu}^T)} \right\rangle$$

$$= \tau^{-1} \sum_\nu \left\langle \frac{\mu_{S\nu}^3\ \omega_S^2\ \omega_I^2\ c\epsilon_0 r_0^2\ |A_{I\lambda}|^2\ |\underline{e}_{S\nu}^* \cdot (\underline{\underline{I}}-\underline{\underline{\epsilon}}_I)\cdot\underline{e}_{I\lambda}|^2 |\delta n_e^T(\underline{k},\omega)|^2}{4\pi\ \omega_{pe}^4\ (\underline{e}_{S\nu}^* \cdot \underline{\underline{\epsilon}}_S \cdot \underline{e}_{S\nu})} \right\rangle$$

$$= \frac{\langle |\delta n_e^T(\underline{k},\omega)|^2\rangle}{\tau} \sum_\nu \frac{\mu_{S\nu}^3\ \omega_S^2\ \omega_I^2\ C\ \epsilon_0\ r_0^2}{4\pi\ \omega_{pe}^4} \frac{|A_I|^2\ |\underline{e}_{S\nu}^* \cdot (\underline{\underline{I}}-\underline{\underline{\epsilon}}_I)\cdot \underline{e}_I|^2}{e_{S\nu}^* \cdot \underline{\underline{\epsilon}}_S \cdot \underline{e}_{S\nu}} \tag{29}$$

with

$$\underline{k}_{S\nu} = \hat{\underline{k}}_S\ \mu_{S\nu}(\hat{\underline{k}}_S)\ \omega_S/c, \quad \underline{k} = \underline{k}_{S\nu} - \underline{k}_{I\lambda}, \quad \omega = \omega_S - \omega_I\ .$$

Here $r_o = e^2/m_e c^2$ is the classical electron radius.

The spectral density function for density fluctuations in a plasma of volume V is defined (Sheffield, 1975) as

$$S(\underline{k},\omega) = \lim_{V,\tau\to\infty} \left[\frac{\langle |\delta n_e^T(\underline{k},\omega)|^2\rangle}{V\ \tau\ n_e} \right]. \tag{30}$$

Note that this quantity has dimensions of (angular frequency)$^{-1}$. The function has been calculated and is discussed briefly in Section (6).

Several definitions of the differential scattering cross-section have been used in the literature. We consider the scattering from an incident wave of polarization $\underline{e}_{I\lambda}$ into a scattered wave of polarization $\underline{e}_{S\nu}$. We shall first use the relationship

$$\frac{d^2P_S}{d\Omega_{kS}d\omega_S} = W_{I\lambda}\ \frac{d^2\Sigma_{\lambda\nu}}{d\Omega_{kS}d\omega_S}\ V\ n_e\ , \tag{31}$$

where $W_{I\lambda}$ is the incident flux per unit area. Then the differential scattering cross-section is defined per unit wave vector solid angle and per unit angular frequency for a single polarization ν of the scattered radiation:

$$\frac{d^2\Sigma_{\lambda\nu}}{d\Omega_{kS}d\omega_S} = \frac{\mu_{S\nu}^3\,\omega_S^2\,\omega_I^2\,c\,\epsilon_0\,r_0^2\,|A_{I\lambda}|^2\,|\underline{e}_{S\nu}^*\cdot(\underline{\underline{I}}-\underline{\underline{\epsilon}}_I)\cdot\underline{e}_{I\lambda}|^2\,S(\underline{k},\omega)}{4\pi\,\omega_{pe}^4\,(\underline{e}_{S\nu}^*\cdot\underline{\underline{\epsilon}}_S\cdot\underline{e}_{S\nu})\,W_{I\lambda}} . \tag{32}$$

The time averaged incident flux per unit area, $W_{I\lambda}$, is given by expression (5):

$$\underline{W}_{I\lambda} = \tfrac{1}{4}\,[\,\underline{E}_{I\lambda}^*\times\underline{H}_{I\lambda}+\underline{E}_{I\lambda}\times\underline{H}_{I\lambda}^*\,]$$

$$= \tfrac{1}{4}\,\mu_{I\lambda}\,\epsilon_0\,c\,|A_{I\lambda}|^2\,[\,2\,\hat{\underline{k}}_I\,|\underline{e}_{I\lambda}|^2-\underline{e}_{I\lambda}^*\,(\hat{\underline{k}}_I\cdot\underline{e}_{I\lambda})-\underline{e}_{I\lambda}\,(\hat{\underline{k}}_I\cdot\underline{e}_{I\lambda}^*)\,] . \tag{33}$$

This expression may be rewritten more simply by taking the component of $\underline{W}_{I\lambda}$ along $\hat{\underline{k}}_I$ and dividing by $\cos\delta_{I\lambda}$, $\delta_{I\lambda}$ being the angle between $\hat{\underline{k}}_I$ and the direction of ray propagation:

$$W_{I\lambda} = \frac{\mu_{I\lambda}\epsilon_0 c\,|A_{I\lambda}|^2}{2\cos\delta_{I\lambda}}\left[\,|\underline{e}_{I\lambda}|^2-|\underline{e}_{I\lambda}\cdot\hat{\underline{k}}_I|^2\,\right] . \tag{34}$$

Thus

$$\frac{d^2\Sigma_{\lambda\nu}}{d\Omega_{kS}d\omega_S} = \frac{\mu_{S\nu}^3\,\omega_S^2\,\omega_I^2\,r_0^2\,|\underline{e}_{S\nu}^*\cdot(\underline{\underline{I}}-\underline{\underline{\epsilon}}_I)\cdot\underline{e}_{I\lambda}|^2\,S(\underline{k},\omega)\cos\delta_{I\lambda}}{2\pi\,\mu_{I\lambda}\,\omega_{pe}^4\,(\underline{e}_{S\nu}^*\cdot\underline{\underline{\epsilon}}_S\cdot\underline{e}_{S\nu})\,[|\underline{e}_{I\lambda}|^2-|\underline{e}_{I\lambda}\cdot\hat{\underline{k}}_I|^2]} . \tag{35}$$

This expression is the same as that given by Akhiezer et al. (1962), except that in their treatment $W_{I\lambda}$ was taken to be only the component of the flux along $\hat{\underline{k}}_I$, so the $\cos\delta_{I\lambda}$ term was not included.

Hutchinson (1988) has pointed out that (35) may be written in a more symmetrical form. The field $\underline{e}_{I\lambda}$ satisfies the dispersion relation

$$k_{I\lambda}^2 \left[\underline{e}_{I\lambda} - \hat{\underline{k}}_I \left(\hat{\underline{k}}_I \cdot \underline{e}_{I\lambda} \right) \right] - \left(\frac{\omega_I}{c} \right)^2 \left(\underline{\underline{\epsilon}}_I \cdot \underline{e}_{I\lambda} \right) = 0 ,$$

so

$$\underline{e}_{I\lambda}^* \cdot \underline{\underline{\epsilon}}_I \cdot \underline{e}_{I\lambda} = \frac{k_{I\lambda}^2 c^2}{\omega_I^2} \underline{e}_I^* \cdot \left[\underline{e}_{I\lambda} - \hat{\underline{k}}_I \left(\hat{\underline{k}}_I \cdot \underline{e}_{I\lambda} \right) \right]$$

$$= \mu_{I\lambda}^2 \left[|\underline{e}_{I\lambda}|^2 - |\underline{e}_{I\lambda} \cdot \hat{\underline{k}}_I|^2 \right] . \qquad (36)$$

Thus

$$\frac{d^2\Sigma_{\lambda\nu}}{d\Omega_{RS} d\omega_S} = \frac{\mu_{S\nu}^3 \mu_{I\lambda} \omega_S^2 \omega_I^2 r_0^2 |\underline{e}_{S\nu}^* \cdot (\underline{\underline{I}} - \underline{\underline{\epsilon}}_I) \cdot \underline{e}_{I\lambda}|^2 S(\underline{k},\omega) \cos \delta_{I\lambda}}{2\pi \omega_{pe}^4 \left(\underline{e}_{S\nu}^* \cdot \underline{\underline{\epsilon}}_S \cdot \underline{e}_{S\nu} \right) \left(\underline{e}_{I\lambda}^* \cdot \underline{\underline{\epsilon}}_I \cdot \underline{e}_{I\lambda} \right)} . \qquad (37)$$

Alternatively, the differential scattering cross-section may be defined per unit ray solid angle, Ω_{rS}, so

$$\frac{d^2P_S}{d\Omega_{rS} d\omega_S} = W_{I\lambda} \frac{d^2\sigma_{\lambda\nu}}{d\Omega_{rS} d\omega_S} V n_e . \qquad (38)$$

Then

$$\frac{d^2\sigma_{\lambda\nu}}{d\Omega_{rS} d\omega_S} = \frac{d^2\Sigma_{\lambda\nu}}{d\Omega_{kS} d\omega_S} \frac{d\Omega_{kS}}{d\Omega_{rS}} ,$$

and since from (16)

$$\frac{d\Omega_{kS}}{d\Omega_{rS}} = \frac{\cos \delta_{S\nu}}{C_{S\nu}} ,$$

from (35)

$$\frac{d^2\sigma_{\lambda\nu}}{d\Omega_{rS}\,d\omega_S} = \frac{\mu_{S\nu}^3\,\omega_S^2\,\omega_I^2\,r_0^2\,|\underline{e}_{S\nu}^*\cdot(\underline{\underline{I}}-\underline{\underline{\epsilon}}_I)\cdot\underline{e}_{I\lambda}|^2\,S(\underline{k},\omega)\,\cos\delta_{I\lambda}\cos\delta_{S\nu}}{2\pi\,\mu_{I\lambda}\cdot\omega_{pe}^4\,(\underline{e}_{S\nu}^*\cdot\underline{\underline{\epsilon}}_S\cdot\underline{e}_{S\nu})\,[|\underline{e}_{I\lambda}|^2-|\underline{e}_{I\lambda}\cdot\hat{\underline{k}}_I|^2]\cdot C_{S\nu}} \quad . \tag{39}$$

This is the expression given by Bretz (1987), except that his cross-section is defined per Hz and $\underline{\underline{\epsilon}}_I$ in the numerator is misprinted as $\underline{\underline{\epsilon}}_S$. A similar expression is given by Simonich and Yeh (1971).

Making use of (36) again and recalling that $C_{S\nu} = \frac{\mu_{S\nu}^2}{\mu_{rS\nu}^2}$ a more symmetrical form for (39) is obtained:

$$\frac{d^2\sigma_{\lambda\nu}}{d\Omega_{rS}\,d\omega_S} = \frac{\mu_{S\nu}\,\mu_{I\lambda}\,\omega_S^2\,\omega_I^2\,r_0^2\,|\,\underline{e}_{S\nu}^*\cdot(\underline{\underline{I}}-\underline{\underline{\epsilon}}_I)\cdot\underline{e}_{I\lambda}\,|^2\,S(\underline{k},\omega)\,\cos\delta_{I\lambda}\cos\delta_{Sr}\,\mu_{rS\nu}^2}{2\pi\,\omega_{pe}^4\,(\underline{e}_{S\nu}^*\cdot\underline{\underline{\epsilon}}_S\cdot\underline{e}_{S\nu})\,(\underline{e}_{I\lambda}^*\cdot\underline{\underline{\epsilon}}_I\cdot\underline{e}_{I\lambda})} \quad . \tag{40}$$

Explicit expressions for terms in expression (37) and (40) are given in Appendix 1.

5. THE SCATTERED POWER ACCEPTED BY A HETERODYNE RECEIVER

Siegman (1966) showed that if the antenna pattern of an optical heterodyne receiver has a single main lobe subtending a solid angular field of Ω steradians, then the effective aperture area A for sources at wavelength λ inside this field is given by

$$A\,\Omega = \lambda^2 \quad . \tag{41}$$

In this section we make use of this result in the geometrical optics approximation to find the scattered power accepted in a single mode by the receiver antenna.

Consider first a narrow pencil of radiation in a loss-free, homogeneous, isotropic medium, connecting two planes normal to the axis with elementary areas A_1 and A_2 separated by a distance R (see Figure 2). The solid angle subtended by dA_2 at a point on dA_1 is $d\Omega_1$, while that subtended by dA_1 at dA_2 is $d\Omega_2$. Then

$$d\Omega_1 = \frac{dA_2}{R} \quad , \quad d\Omega_2 = \frac{dA_1}{R} \quad ,$$

and so

$$dA_1 d\Omega_1 = dA_2 d\Omega_2 = \frac{dA_1 dA_2}{R} \tag{42}$$

(this quantity is known as the étendue of the system).

The specific intensity I of the radiation in the pencil is defined as the power per unit area per unit solid angle per unit bandwidth. Thus if the power transmitted along the pencil in bandwidth $d\omega$ is dP,

$$I = \frac{dP}{dA\ d\Omega\ d\omega} \quad . \tag{43}$$

In a slowly-varying, inhomogeneous, lossless medium it can be shown (Bekefi (1966), p.31) that

$$\frac{I}{\mu^2} = \text{const.} \tag{44}$$

Thus, since neither dP nor $d\omega$ change along the pencil,

$$dA\ d\Omega\ \mu^2 = \text{const.} \tag{45}$$

In an anisotropic medium μ must be replaced by μ_r, the ray refractive index, so

$$dA\ d\Omega_r\ \mu_r^2 = \text{const} \ , \tag{46}$$

$d\Omega$ being the element of ray solid angle.

To simplify the discussion we consider a scattering experiment in which the antenna patterns of both the incident and the accepted, scattered radiation have square cross sections in the scattering volume, with side a (Figure 3). The angle between the incident and scattered ray directions is θ_r (and is not in general equal to the "scattering angle" θ between $\underline{k}_I$ and k_S). Then the volume of the region of interaction is

$$V = \frac{a^3}{\sin \theta_r} \tag{47}$$

while the area of each beam is

$$A = a^2 \ . \tag{48}$$

If the total incident beam power is P_I, the scattered power in the receiver antenna pattern at the scattering region per unit ray solid angle and bandwidth is, from (38),

$$\left(\frac{d^2P_S}{d\Omega_r \, d\omega} \right)_V = \frac{P_I}{A} \, V \, n_e \frac{d^2\sigma}{d\Omega_r \cdot d\omega}$$

$$= P_I \frac{a}{\sin \theta_r} n_e \frac{d^2\sigma}{d\Omega_r \cdot d\omega} \ . \tag{49}$$

We shall assume that the radiation flux is uniform across each beam. Then the specific intensity of the scattered radiation in the receiver antenna pattern at the scattering region is

$$(I_S)_V = \frac{1}{a^2} \left(\frac{d^2P_S}{d\Omega_r \, d\omega} \right)_V = P_I \frac{n_e}{a \sin \theta_r} \frac{d^2\sigma}{d\Omega_r \, d\omega} \ . \tag{50}$$

In the scattering experiment the scattered radiation propagates away from the scattering region and finally reaches the receiver antenna, which is outside the plasma. Provided the properties of the plasma vary sufficiently slowly, so that the whole antenna pattern may be regarded as a simple pencil, we may write, from (46),

$$A \, \Omega_r \, \mu_{rS}^2 = \text{const} \ ,$$

$$\frac{(A\Omega_r)_{\text{antenna}}}{(A\Omega_r)_V} = \frac{(\mu_{rS}^2)_V}{(\mu_{rS}^2)_{\text{antenna}}} \ . \tag{51}$$

At the antenna, in free space, $\mu_{rS}^2 = 1$, and from (41)

$$(A\Omega_r)_{antenna} = \lambda_{SO}^2 \quad , \tag{52}$$

λ_{SO} being the free space wavelength of the scattered radiation.

Then

$$(A\Omega_r)_V = \frac{\lambda_{SO}^2}{(\mu_{rS}^2)_V} \, . \tag{53}$$

The power received by the antenna in the single scattered mode, in angular frequency bandwidth $\Delta\omega$, is thus given by

$$P_S = (I_S)_V \, (A \cdot \Omega_r)_V \, \Delta\omega$$

so from (50)

$$P_S = P_I \frac{n_e}{a \sin\theta_r} \frac{d^2\sigma}{d\Omega_r \, d\omega} \frac{\lambda_{SO}^2}{(\mu_{rS}^2)_V} \Delta\omega \, . \tag{54}$$

Instead of using the differential scattering cross-section per unit ray solid angle we can make use of the cross-section per unit wave vector solid angle,

$$\frac{d^2\Sigma}{d\Omega_k \, d\omega} = \frac{d^2\sigma}{d\Omega_r \, d\omega} \frac{C_S}{\cos\delta_S} = \frac{d^2\sigma}{d\Omega_r \, d\omega} \frac{\mu_S^2}{(\mu_{rS}^2)_V \cos\delta_S} \, . \tag{55}$$

Then

$$P_S = P_I \frac{n_e}{a \sin\theta_r} \frac{d^2\Sigma}{d\Omega_k \, d\omega} \frac{\lambda_{SO}^2}{(\mu_S^2)_V} (\cos\delta_S)_V \Delta\omega \, . \tag{56}$$

A similar conclusion was reached by Hutchinson (1987).

From (54) and (40) we find that if the incident power with polarization λ is $P_{I\lambda}$, the detectable scattered power with polarization ν in bandwidth $\Delta\omega$ rad.s^{-1} at the antenna of the heterodyne receiver is

$$P_{S\nu} = P_{I\lambda} \, \Delta\omega \, r_0^2 \, \lambda_{So}^2 \, \omega_S^2 \, \omega_I^2 \, \frac{1}{2\pi} \, x$$

$$\times \left[\frac{n_e}{\omega_{pe}^4} \; \frac{\mu_{S\nu}\,\mu_{I\lambda}\,|\underline{e}^*_{S\nu}\cdot(\underline{\underline{I}}-\underline{\underline{\epsilon}}_I)\cdot\underline{e}_{I\lambda}|^2}{(\underline{e}^*_{S\nu}\cdot\underline{\underline{\epsilon}}_S\cdot\underline{e}_{S\nu})\;(\underline{e}^*_{I\lambda}\cdot\underline{\underline{\epsilon}}_I\cdot\underline{e}_{I\lambda})} \qquad \frac{\cos\delta_{I\lambda}\;\cos\delta_{S\nu}}{a\,\sin\theta_r}\;\; S(\underline{k},\omega) \right]_V , \tag{57}$$

all quantities in the large brackets being evaluated at the scattering volume.

If a more realistic antenna pattern is used in the calculation, expressions (54), (56) and (57) will have to be modified, replacing (a) by some appropriate beam width parameter, but the functional dependence should be unchanged.

If the effects of refraction and polarization are ignored the detectable scattered power may be written as

$$Q_S = \frac{P_{I\lambda}\,\Delta\omega\; r_0^2\;\; \lambda_{So}^2\; n_e}{2\pi\; a\,\sin\theta_r}\;\; S(\underline{k},\omega) \quad . \tag{58}$$

We introduce the geometrical form factor $G_{\lambda\nu}$, defined by

$$P_{S\nu} = G_{\lambda\nu}\; Q_S \; . \tag{59}$$

$G_{\lambda\nu}$ is similar to, but not the same as, the factor Γ defined by Bretz (1987). It is a useful measure of the effects of polarization and refraction on the detectable scattered power. Provided the same form of $S(\underline{k},\omega)$ is used in both (57) and (58),

$$G_{\lambda\nu} = \frac{\omega_S^2\;\omega_I^2}{\omega_{pe}^4}\;\; \frac{\mu_{S\nu}\,\mu_{I\lambda}\,|\underline{e}^*_{S\nu}\cdot(\underline{\underline{I}}-\underline{\underline{\epsilon}}_I)\cdot\underline{e}_{I\lambda}|^2\cos\delta_{I\lambda}\cos\delta_{S\nu}}{(\underline{e}^*_{S\nu}\cdot\underline{\underline{\epsilon}}_S\cdot\underline{e}_{S\nu})\;(\underline{e}^*_{I\lambda}\cdot\underline{\underline{\epsilon}}_I\cdot\underline{e}_{I\lambda})} \quad . \tag{60}$$

6. THE SCATTERING SPECTRAL FUNCTION $S(k,\omega)$

The function $S(\underline{k},\omega)$ for a magnetized plasma is discussed in detail by Sheffield (1975). Following the work of Vahala *et al.* (1986), a computer code has been prepared which gives $S(\underline{k},\omega)$ for a wide range of wavelengths and plasma parameters (Hughes and Smith (1988)). In the earlier versions of the code it was assumed that $|\underline{k}_{S\nu}| \approx |\underline{k}_{I\lambda}|$, both in deriving $|\underline{k}| = |\underline{k}_{S\nu} - \underline{k}_{I\lambda}| \approx 2k_{I\lambda}\sin\frac{\Theta}{2}$ for a scattering angle Θ, and for determining the angle ϕ between $\underline{k}$ and $\underline{B}$. In the present version the local values of $\underline{k}_{I\lambda}$, $\underline{k}_{S\nu}$ and $\underline{B}$ in the scattering region are

entered. Then θ and $|\underline{k}|=[k_{S\nu}^2+k_{I\lambda}^2-2k_{S\nu}k_{I\lambda}\cos\theta]^{\frac{1}{2}}$ are calculated accurately, together with the angle ϕ.

The code includes the effects of several different ion species with different Maxwellian distributions, and fast ions (e.g. alpha particles) with a "slow-down" distribution. Relativistic effects have not yet been included.

In a Thomson scattering experiment it will be necessary to compare the observed spectrum with calculated spectra to obtain information about the particle velocity distribution function. This will require a knowledge of $G_{\lambda\nu}$ as well as $S(\underline{k},\omega)$.

7. CALCULATIONS OF $G_{\lambda\nu}$

We have calculated values of $G_{\lambda\nu}$ for a variety of scattering situations, using expressions given in Appendix 1. As an example we give results for the scattering geometry shown in Figure 4. Here $\underline{k}_I$, $\underline{k}_S$ and $\underline{B}$ are coplanar, so $\chi = 0$. The scattering vector $\underline{k} = \underline{k}_S - \underline{k}_I$ will be approximately antiparallel to $\underline{B}$. The other fixed parameters are $B = 3.4$ T and $f_I = 140$ GHz. The scattered spectrum is considered in the frequency range $135 < f_S < 145$ GHz. Values of $G_{\lambda\nu}$ are shown for several electron densities in the range $2 \times 10^{19}\ m^{-3} \leq n_e \leq 1.5 \times 10^{20}\ m^{-3}$ in Figures 5(a) to 5(g), for O mode to O mode, O to X, X to O and X to X scattering.

i) O to O Scattering

The results (Figure 5(a)) are straightforward. Except at the lowest densities, the geometrical form factor is somewhat larger than unity.

ii) O to X Scattering

When either or both of the waves are X mode the scattering may be strongly influenced by resonance or cut-off. It is helpful to refer to Figure 6, which shows the upper hybrid resonance frequency, given by

$$(2\pi f_{UH})^2 = \frac{\omega_{ce}^2 + \omega_{pe}^2 + [(\omega_{ce}^2 + \omega_{pe}^2)^2 - 4\omega_{pe}^2\,\omega_{ce}^2\cos^2\phi]^{\frac{1}{2}}}{2} \qquad (61)$$

and the X mode R cut-off frequency, given by

$$2\pi f_R = [(\frac{\omega_{ce}}{2})^2 + \omega_{pe}^2]^{\frac{1}{2}} + \frac{\omega_{ce}}{2} \qquad (62)$$

as functions of density for the conditions considered (the cut-off is independent of ϕ and the upper hybrid frequency varies only slightly with ϕ for $60 < \phi < 120°$). There can be no scattered X mode in the frequency range 135 to 145 GHz if the electron density n_e is between 9×10^{19} m^{-3} and 1.2×10^{20} m^{-2}.

Figure 5(b) shows that at low densities ($2 \times 10^{19} \lesssim n_e \lesssim 6 \times 10^{19}$ m^{-3}) G_{+-} is small, between 0.2 and 0.4, and decreases as n_e is increased. When the density is increased further the R cut-off moves through the scattered frequency range of interest and a narrow spike in G_{+-} appears close to the cut-off frequency.

Figure 5(c) shows the reappearance of scattered X-mode radiation when the density is increased above $n_e = 1.2 \times 10^{20}$ m^{-3}. The upper hybrid resonance enters and passes through the frequency region of the calculations. Larger spikes in G_{+-}appear close to the resonance.

iii) X to O Scattering

In this case the input X mode is cut off in the density range 8×10^{19} $m^{-3} \lesssim n_e \lesssim 1.35 \times 10^{20}$ m^{-3}. At low densities (Figure 5(d)) the values of G_{-+} are small and similar to those for O to X scattering. There are no spikes, either at $n_e = 7 \times 10^{20}$ m^{-3} or at $n_e = 1.4$ or 1.5×10^{20} m^{-3} (Figure 5(e)).

iv) X to X Scattering

Again, the input X mode is cut off for 8×10^{19} $m^{-3} \lesssim n_e \lesssim 1.35 \times 10^{20}$ m^{-3}. In this case, Figure 5(f) shows that G_{--} is greater than 5 even at the lowest density ($n_e = 2 \times 10^{19}$ m^{-3}) and increases as n_e is increased. At $n_e = 7 \times 10^{19}$ m^{-3} a large spike appears near the R cut-off frequency, with G_{--} rising to more than 300. At the highest densities, Figure 5(g) shows very large spikes near the upper hybrid resonance, with $G_{--} > 2000$.

It must be stressed that the calculations are for fixed $\hat{k}_I$, $\hat{k}_S$, ϕ_I and ϕ_S. The ray

directions can be very different to the $\underline{k}$ directions for the X mode near the upper hybrid frequency, where large values of the refractive index may be encountered. For example, for the conditions considered, with $n_e = 1.5 \times 10^{20}$ m^{-3}, the X mode refractive index at 143 GHz is about 4 and the angle δ between the ray and $\underline{k}$ directions is 75°. In a scattering experiment the antennas will be adjusted so that their patterns intersect in a given region of the plasma for selected incident and scattered polarization. If one of the polarizations is changed the corresponding ray path through the plasma will also change, so the scattering volume will move and may vanish. In general, therefore, it is very unlikely that the same $\hat{\underline{k}}_I$, $\hat{\underline{k}}_S$, ϕ_I and ϕ_S will be appropriate for different pairs of polarizations for fixed antenna orientations.

The large values of G at frequencies near the X mode poles suggest that the substantial enhancement of the detected power might be used to advantage here. However, the severe distortion of the ray trajectories and the sensitivity to changes in the plasma parameters would make it extremely difficult to extract reliable information about $S(\underline{k},\omega)$ from experimental measurements in such conditions.

It should also be noted that we have ignored the question of access. For example, in a tokamak plasma the upper hybrid resonance is not accessible to X-mode radiation from outside the plasma, which will either be strongly absorbed en route by the electron cyclotron resonant layer or reflected by the R cut-off layer.

8. DETERMINATION OF SCATTERING PARAMETERS

In order to make use of the results given above in a millimetre wave scattering experiment we need to know the scattering geometry in detail, together with the plasma parameters n_e, T_e and $\underline{B}$ in the scattering volume. A ray tracing code is essential both for setting up and for interpreting an experiment, and the ray tracing can only be done if the plasma magnetic equilibrium and electron density profile are adequately known.

The positions of the transmitting and receiving antennas will be determined by the availability of ports in the tokamak vacuum vessel. The orientations of the antennas must be adjustable.

8.1 Setting Up

The procedure for setting up an experiment will probably be similar to the following:

(1) Decide where in the plasma the centre of the scattering volume, C, is to be located.

(2) For the expected plasma equilibrium and density profile find by iteration, using the ray tracing code, the orientation of the transmitter antenna that carries the central ray of the antenna pattern for a given (O or X) polarization λ and frequency ω_I to point C.

(3) Similarly find the orientation of the receiver antenna that brings the central ray for polarization ν and frequency ω_S to point C.

8.2 Interpretation

After the experiment the actual plasma equilibrium and density profile measured at the time should be used for further ray tracing.

(1) For the known orientation of the transmitter antenna, trace a group of rays representing the antenna pattern through the plasma at frequency f_I.

(2) Similarly, follow a group of rays representing the detector antenna pattern through the plasma at frequency f_S.

(3) From the intersection of the two antenna patterns define the actual scattering volume and its (weighted) centre C′. Find local values of n_e, T_e and $\underline{B}$.

(4) Use the ray tracing code to follow transmitted and detected rays to C′, and find $\underline{k}_{I\lambda}$ and $\underline{k}_{S\nu}$.

All the parameters required to calculate G are now known (ϕ_I, ϕ_S, ρ_I, ρ_S, δ_I, δ_S, χ, θ_r, n_e, B). Also θ, k, ϕ, n_e and T_e are available for use in $S(\underline{k},\omega)$. Provided

the scattered spectrum is not too broad and the scattering volume is not too extensive the procedure described above should be adequate. If the scattered spectrum is very broad it may be necessary to repeat the calculations for different scattered frequencies. Also, the extent of the scattering volume will determine the variation in each of the parameters required and thus the accuracy of the calculated velocity distributions. It should be noted that if the scattered spectrum is broad the shape and position of the scattering volume may vary significantly with the scattered frequency, with consequential changes in n_e, $\underline{B}$, T_e, and all the other parameters. It is possible that the relatively straightforward procedure in (1) to (4) above will be sufficiently accurate for practical purposes, but the frequency dependence indicated should be investigated for some representative conditions to establish the accuracy of the data.

The observed scattered spectrum may now be interpreted in terms of particle distribution functions and densities.

Regarding steps (1) and (2), Bretz (1988) has remarked that the usual ray tracing calculations do not describe the propagation of the focused, near-Gaussian beams which are likely to be used in experiments. A Gaussian beam in an isotropic medium can be simulated by making use of the straight line generators of the usual hyperboloidal surface. This approach has been used successfully to calculate the approximate shapes of focused microwave antenna patterns in JET plasmas, by following the generators with a ray tracing code (Hughes et al. 1989). Although the generators do not accurately represent propagation directions they do provide useful approximate indications of the beam profile and the shape of the scattering volume.

ACKNOWLEDGEMENTS

We are grateful to I H Hutchinson of MIT for a private communication on this subject which led us to carry out the work reported here, and for reading the paper in draft and making valuable suggestions for improvement. We thank N Bretz of Princeton Plasma Physics Laboratory, D Bartlett and A E Costley, who also read the draft, for their helpful comments; D A Boyd of the University of Maryland, J A Hoekzema and P E Stott of JET for enlightening discussions and encouragement, and the JET Project for support.

REFERENCES

Airoldi, A., Orefice, A. and Ramponi, G. 1988 Report FP88/8, Istituto di Fisica del Plasma, ENEA Milan.

Akhiezer, A.I., Akhiezer, I.A. and Sitenko, A.G. 1962 Sov. Phys. JETP 14, 462.

Batchelor, D.B., Goldfinger, R.C. and Weitzner, H. 1980 IEEE Trans. on Plasma Science, P5-8, 78.

Bekefi, G. 1966 "Radiation Processes in Plasmas", J Wiley.

Boyd, D.A. 1985 Proc. 5th Int. Workshop on Electron Cyclotron Emission and Electron Cyclotron Heating, San Diego, p.77.

Boyd, D.A. 1988 Laboratory for Plasma Research, University of Maryland, private communication.

Bretz, N. 1987 J. Plasma Physics 38, 79.

Bretz, N. 1988 Plasma Physics Laboratory, Princeton University, private communication.

Heald, M.A. and Wharton, C.B. 1965 "Plasma Diagnostics with Microwaves", J Wiley.

Hughes, T.P. et al. 1989 Proc. 16th EPS Conference on Controlled Fusion and Plasma Physics, Venice.

Hughes, T.P., and Smith, S.R.P. 1988 Nuclear Fusion 28, 1458.

Hutchinson, I.H. 1979 Plasma Physics 21, 1043.

Hutchinson, I.H. 1987 Massachusetts Institute of Technology, private communication.

Hutchinson, I.H. 1988 private communication.

Kritz, A.H., et al. 1983 Princeton Plasma Physics Laboratory Report PPPL-1980.

Mercier, R.P. 1964 Proc. Phys. Soc. 83, 811.

Sheffield, J. 1975 "Plasma Scattering of Electromagnetic Radiation", Academic Press.

Siegman, A.E. 1966 Proc. IEEE 54, 1350.

Simonich, D.M. and Yeh, K.C. 1971 Ionosphere Radio Laboratory Report 42, University of Illinois.

Sitenko, A.B., 1967 "Electromagnetic Fluctuations in Plasma", Academic Press.

Stix, T.H., 1962 "The Theory of Plasma Waves", McGraw Hill.

Vahala, L., Vahala, G., and Sigmar, D.J. 1986 Nuclear Fusion 26, 51: see also Nuclear Fusion 28, 1595 (1988).

Woskoboinikow, P., Cohn, D.R. and Temkin, R.J. 1983 Int. J. of Infrared and Millimeter Waves 4, 205.

APPENDIX 1

EXPLICIT EXPRESSIONS FOR FACTORS IN THE SCATTERING CROSS-SECTIONS

Following Akhiezer et al. (1962) it is convenient to introduce the notation

$$R_{\lambda\nu} = \frac{\mu_{S\nu}^3}{\mu_{I\lambda}\,(|\underline{e}_{I\lambda}|^2 - |\underline{e}_{I\lambda}\cdot\hat{\underline{k}}_I|^2)\,(\underline{e}_{S\nu}\cdot\underline{\underline{\epsilon}}_S\cdot\underline{e}_{S\nu})}$$

$$= \frac{\mu_{S\nu}^3\,\mu_{I\lambda}}{(\underline{e}^*_{S\nu}\cdot\underline{\underline{\epsilon}}_S\cdot\underline{e}_{S\nu})\,(\underline{e}^*_{I\lambda}\cdot\underline{\underline{\epsilon}}_I\cdot\underline{e}_{I\lambda})}\ , \tag{A1}$$

$$\xi_{\lambda\nu} = \underline{e}^*_{S\nu}\cdot(\underline{\underline{I}} - \underline{\underline{\epsilon}}_I)\cdot\underline{e}_{I\lambda}\ . \tag{A2}$$

Then from expression (37),

$$\frac{d^2\Sigma_{\lambda\nu}}{d\Omega_{kS}d\omega_S} = \frac{r_0^2}{2\pi}\,\frac{\omega_S^2\,\omega_I^2}{\omega_{pe}^4}\,R_{\lambda\nu}\,|\xi_{\lambda\nu}|^2\cos\delta_{I\lambda}\,S(\underline{k},\omega) \tag{A3}$$

or if the angular frequency bandwidth $d\omega_S$ and the scattered angular frequency shift ω are replaced by df_S (Hz) and f(Hz),

$$\frac{d^2\Sigma_{\lambda\nu}}{d\Omega_{kS}df_S} = r_0^2\,\frac{\omega_S^2\,\omega_I^2}{\omega_{pe}^4}\,R_{\lambda\nu}\,|\xi_{\lambda\nu}|^2\,\cos\delta_{I\lambda}\,S'(\underline{k},f)\ . \tag{A4}$$

Similarly, from (39),

$$\frac{d^2\,\sigma_{\lambda\nu}}{d\Omega_{rS}df_S} = r_0^2\,\frac{\omega_S^2\,\omega_I^2}{\omega_{pe}^4}\,R_{\lambda\nu}\,|\xi_{\lambda\nu}|^2\,\frac{\cos\delta_{I\lambda}\cos\delta_{S\nu}}{C_{S\nu}}\,S'(\underline{k},f)\ . \tag{A5}$$

The factor $G_{\lambda\nu}$ given in expression (60) becomes

$$G_{\lambda\nu} = \frac{\omega_S^2\ \omega_I^2}{\omega_{pe}^4}\ R_{\lambda\nu}\ \ |\xi_{\lambda\nu}|^2\ \ \frac{\cos\delta_{I\lambda}\ \cos\delta_{S\nu}}{\mu_{S\nu}^2}\ . \qquad \text{(A6)}$$

The terms cos $\delta_{I\lambda}$, cos $\delta_{S\nu}$ are obtained from expression (9). The spectral density function S,S′ will not be discussed further here. The square of the classical electron radius is $r_0^2 = 7.941 \times 10^{-30}\ m^2$.

We shall take the direction of the wave vector of the incident wave, $\hat{\underline{k}}_I$, to lie in the (x,z) plane at an angle ϕ_I to the z-axis and $\underline{B}$ (see Figure 7). Then from (4), for polarization $\lambda = \pm 1$,

$$\underline{E}_{I\lambda} = A_{I\lambda}\ \underline{e}_{I\lambda}\ \exp\ [\ i(\underline{k}_{I\lambda} \cdot \underline{r} - \omega_I t)\ ]\ ,$$

with

$$\underline{e}_{I\lambda} = \{\ 1,\ \frac{i\epsilon_{2I}}{\mu_{I\lambda}^2 - \epsilon_{1I}}\ ,\ \frac{\mu_{I\lambda}^2 \cos\phi_I\ \sin\phi_I}{\mu_{I\lambda}^2 \sin^2\phi_I - \epsilon_{3I}}\ \}\ , \qquad \text{(A7)}$$

where

$$\mu_{I\lambda}^2 = 1 - \frac{2\alpha_I\ (1 - \alpha_I)}{2(1 - \alpha_I) - \beta_I \sin^2\phi_I + \lambda\gamma_I^{1/2}}\ ,$$

$$\gamma_I = (\beta_I \sin^2\phi_I)^2 + 4\beta_I (1-\alpha_I)^2 \cos^2\phi_I$$

and α_I, β_I, ϕ_I, ϵ_{1I}, etc are evaluated at $\omega = \omega_I$.

When $\phi_I = \frac{\pi}{2}$, for the O mode

$$\underline{e}_{I+}\ (\phi_I = \tfrac{\pi}{2}) = \{\ 0,0,1\ \}$$

and for the X mode

$$\underline{e}_{I-}\ (\phi_I = \tfrac{\pi}{2}) = \{\ 1,\ \frac{-i\epsilon_{1I}}{\epsilon_{2I}}\ ,\ 0\ \}\ . \qquad \text{(A7a)}$$

The direction of the scattered wave vector, $\hat{\underline{k}}_S$, will be taken to lie at an angle ϕ_S to the z-axis and $\underline{B}$. The angle between the ($\hat{\underline{k}}_I$, $\underline{B}$) and ($\hat{\underline{k}}_S$, $\underline{B}$) planes will be denoted by χ (see Figure 7). Then for polarization ν,

$$\underline{E}_{S\nu} = A_{S\nu} \; \underline{e}_{S\nu} \exp \left[i(\underline{k}_{S\nu} \cdot \underline{r} - \omega_S t) \right]$$

with

$$\left[\underline{e}_{S\nu} \right] = \begin{bmatrix} \cos\chi & -\sin\chi & 0 \\ \sin\chi & \cos\chi & 0 \\ 0 & 0 & 1 \end{bmatrix} \begin{bmatrix} 1 \\ \dfrac{i\epsilon_{2S}}{\mu_{S\nu}^2 - \epsilon_{1S}} \\ \dfrac{\mu_{S\nu}^2 \cos\phi_S \sin\phi_S}{\mu_{S\nu}^2 \sin^2\phi_S - \epsilon_{3S}} \end{bmatrix}$$

$$= \left\{ \cos\chi - \frac{i\epsilon_{2S}\sin\chi}{\mu_{S\nu}^2 - \epsilon_{1S}} \;,\; \sin\chi + \frac{i\epsilon_{2S}\cos\chi}{\mu_{S\nu}^2 - \epsilon_{1S}} \;,\; \frac{\mu_{S\nu}^2 \cos\phi_S \sin\phi_S}{\mu_{S\nu}^2 \sin^2\phi_S - \epsilon_{3S}} \right\}, \quad \text{(A8)}$$

where $\mu_{S\nu}$, ϵ_{1S} etc. are evaluated for ϕ_S and ω_S. When $\phi_S = \pi/2$

$$\underline{e}_{S+\,(\phi=\frac{\pi}{2})} = \{ 0,0,1 \}$$

and

$$\underline{e}_{S-\,(\phi=\frac{\pi}{2})} = \left\{ \cos\chi + i\,\frac{\epsilon_1}{\epsilon_2}\sin\chi,\; \sin\chi - i\,\frac{\epsilon_1}{\epsilon_2}\cos\chi,\; 0 \right\} . \qquad \text{(A8a)}$$

1. EXPRESSION FOR $R_{\lambda\nu}$

In equation (A1) the refractive indices $\mu_{I\lambda}$, $\mu_{S\nu}$ are given by the Appleton-Hartree formula (3), (3a).

From equation (A8),

$$\underline{e}^{*}_{S\nu} \cdot \underline{\underline{\epsilon}}_{S} \cdot \underline{e}_{S\nu} = \epsilon_{1S}\left[1 + \frac{\epsilon_{2S}^{2}}{(\mu_{S\nu}^{2} - \epsilon_{1S})^{2}}\right] + \frac{2\,\epsilon_{2S}^{2}}{\mu_{S\nu}^{2} - \epsilon_{1S}}$$

$$+ \epsilon_{3S}\left[\frac{\mu_{S\nu}^{2} \sin\phi_{S} \cos\phi_{S}}{\mu_{S\nu}^{2} \sin^{2}\phi_{S} - \epsilon_{3S}}\right]^{2}, \qquad \text{(A9)}$$

with a similar expression for $\underline{e}^{*}_{I\lambda} \cdot \underline{\underline{\epsilon}}_{I} \cdot \underline{e}_{I\lambda}$.

Thus

$$R_{\lambda\nu} = \mu_{S\nu}^{3}\,\mu_{I\lambda}\left[\epsilon_{1S}\left[1 + \frac{\epsilon_{2S}^{2}}{(\mu_{S\nu}^{2} - \epsilon_{1S})^{2}}\right] + \frac{2\epsilon_{2S}^{2}}{\mu_{S\nu}^{2} - \epsilon_{1S}}\right.$$

$$\left. + \epsilon_{3S}\left[\frac{\mu_{S\nu}^{2} \sin\phi_{S} \cos\phi_{S}}{\mu_{S\nu}^{2} \sin^{2}\phi_{S} - \epsilon_{3S}}\right]^{2}\right]^{-1} \times$$

$$\left[\epsilon_{1I}\left[1 + \frac{\epsilon_{2I}^{2}}{(\mu_{I\lambda}^{2} - \epsilon_{1I})^{2}}\right] + \frac{2\,\epsilon_{2I}^{2}}{\mu_{I\lambda}^{2} - \epsilon_{1I}} + \epsilon_{3I}\left[\frac{\mu_{I\lambda}^{2} \sin\phi_{I} \cos\phi_{I}}{\mu_{I\lambda}^{2} \sin^{2}\phi_{I} - \epsilon_{3I}}\right]^{2}\right]^{-1}.$$

(A10)

2. EXPRESSION FOR $|\xi_{\lambda\nu}|^{2}$

In equation (A2), from equation (1)

$$(\underline{\underline{I}} - \underline{\underline{\epsilon}}_{I}) = \begin{bmatrix} 1 - \epsilon_{1I} & , & i\epsilon_{2I} & , & 0 \\ -i\epsilon_{2I} & , & 1 - \epsilon_{1I} & , & 0 \\ 0 & , & 0 & , & 1 - \epsilon_{3I} \end{bmatrix} \qquad \text{(A13)}$$

and with $\underline{e}_{I\lambda}$ and $\underline{e}_{S\nu}$ given by (A7) and (A8) we find that

$$|\xi_{\lambda\nu}|^2 = \Bigg[\cos\chi \left[(\epsilon_{1I}-1) + \frac{\epsilon_{2I}^2}{\mu_{I\lambda}^2 - \epsilon_{1I}} + \frac{\epsilon_{2I}\epsilon_{2S}}{\mu_{S\nu}^2 - \epsilon_{1S}} \left(1 + \frac{\epsilon_{1I} - 1}{\mu_{I\lambda}^2 - \epsilon_{1I}}\right)\right]$$

$$+ \left[\frac{\mu_{S\nu}^2 \sin\phi_S \cos\phi_S}{\mu_{S\nu}^2 \sin^2\phi_S - \epsilon_{3S}} \right] \left[\frac{\mu_{I\lambda}^2 \sin\phi_I \cos\phi_I}{\mu_{I\nu}^2 \sin^2\phi_I - \epsilon_{3I}} \right] (\epsilon_{3I} - 1) \Bigg]^2$$

$$+ \left[\sin\chi \left[\epsilon_{2I} + \frac{\epsilon_{2S}(\epsilon_{1I} - 1)}{\mu_{S\nu}^2 - \epsilon_{1S}} + \frac{\epsilon_{2I}(\epsilon_{1I} - 1)}{\mu_{I\lambda}^2 - \epsilon_{1I}} + \frac{\epsilon_{2S}\,\epsilon_{2I}^2}{(\mu_{S\nu}^2 - \epsilon_{1S})(\mu_{I\lambda}^{2} - \epsilon_{1I})} \right] \right]^2 . \tag{A14}$$

3. A NOTE ON NORMALIZATION

Expressions (A12) and (A14) for $R_{\lambda\nu}$ and $|\xi_{\lambda\nu}|^2$ make use of unnormalized polarization vectors $\underline{e}_{I\lambda}$, $\underline{e}_{S\nu}$. However, in the product $R_{\lambda\nu}|\xi_{\lambda\nu}|^2$ which appears in the cross-sections (A3) to (A5) any normalizing factors would cancel out, so $R_{\lambda\nu}|\xi_{\lambda\nu}|^2$ is independent of the magnitudes of $\underline{E}_{I\lambda}$ and $\underline{E}_{S\nu}$ as would be expected. Thus unnormalized polarization vectors may legitimately be used to calculate the scattering cross-section, as in e.g. Sitenko (1967) and Bretz (1987).

4. X TO X MODE SCATTERING WHEN $\underline{k}_S$, $\underline{k}_I$ ARE BOTH PERPENDICULAR TO B

Bretz (1987) has given expressions for X to X mode scattering with $\underline{k}_S$ and $\underline{k}_I$ both perpendicular to $\underline{B}$, so that $\phi_I = \phi_S = \frac{\pi}{2}$. In these calculations unnormalized polarization vectors are used, and it is assumed that $\omega_I \approx \omega_S$, so

$$\epsilon_{1I} = \epsilon_{1S} = \epsilon_1 ,$$

$$\epsilon_{2I} = \epsilon_{2S} = \epsilon_2 ,$$

$$\epsilon_{3I} = \epsilon_{3S} = \epsilon_3 .$$

From (3a), under these conditions ($\underline{k}_I$, $\underline{k}_S \perp \underline{B}$) we find

$$\mu_{I-}^2 = \mu_{S-}^2 = \frac{\epsilon_1^2 - \epsilon_2^2}{\epsilon_1} \quad .$$

From (4a),

$$\underline{e}^*_{S-} \cdot \underline{\underline{\epsilon}}_S \cdot \underline{e}_{S-} = \epsilon_1 \left[\frac{\epsilon_1^2 - \epsilon_2^2}{\epsilon_2^2} \right] = \underline{e}^*_{I-} \cdot \underline{\underline{\epsilon}}_I \cdot \underline{e}_{I-}$$

while from (36)

$$| \underline{e}_{I-} |^2 - | \underline{e}_{I-} \cdot \hat{\underline{k}}_I |^2 = \frac{\underline{e}^*_{I-} \cdot \underline{\underline{\epsilon}}_I \cdot \underline{e}_{I-}}{\mu_{I-}^2} = \frac{\epsilon_1^2}{\epsilon_2^2} \ ,$$

in agreement with Bretz. Also, for the same conditions,

$$|\xi_{--}|^2 = \frac{1}{\epsilon_2^4} \ \{ \cos^2\chi \ [\epsilon_1(\epsilon_1^2 - \epsilon_2^2) - (\epsilon_1^2 + \epsilon_2^2)]^2$$

$$+ \sin^2\chi \ [2\epsilon_1\epsilon_2 - \epsilon_1^2\epsilon_2 + \epsilon_2^3]^2 \ \} \ ,$$

again in agreement with Bretz.

5. EXPRESSION FOR $C_{S\nu}$

Dropping the subscript S, from expression (10) for polarization $\nu = \pm 1$,

$$C_\nu = \left[1 + \sin^2 \delta_\nu - \frac{\cos^2\delta_\nu}{\mu_\nu} \cdot \frac{d^2\mu_\nu}{d\phi^2} \right] \frac{\sin \rho_\nu \cos \delta_\nu}{\sin \phi} \quad . \qquad \text{(A15)}$$

Here δ_ν, the angle between the wave vector and the ray direction, is given by expression (9) and $\rho_\nu = \phi - \delta_\nu$ is the angle between the ray direction and $\underline{B}$. The refractive index μ_ν is given by expression (3), and it is found that

$$\frac{d^2\mu_\nu}{d\phi^2} = \frac{-\nu\beta^2 \ \mu_\nu(1 - \mu_\nu^2)}{\gamma^{3/2}} \ [\ 4(1 - \alpha)^2 \cos^4\phi - \beta \sin^4\phi - \nu(1-3\mu_\nu^2) \sin^2\phi \cos^2\phi \ \gamma^{1/2} \ ] \ . \qquad \text{(A16)}$$

Bekefi (1966) gives the following expression for the ray refractive index:

$$\mu^2_{r\nu} = \left| \frac{\mu_\nu^2 \sin\phi \left[1 + \left(\frac{1}{\mu_\nu}\frac{d\mu_\nu}{d\phi}\right)^2\right]^{1/2}}{\frac{d}{d\phi}\left\{\frac{\cos\phi + \frac{1}{\mu_\nu}\frac{d\mu_\nu}{d\phi}\cdot\sin\phi}{\left[1 + \left(\frac{1}{\mu_\nu}\frac{d\mu_\nu}{d\phi}\right)^2\right]^{1/2}}\right\}} \right| \qquad \text{(A17)}$$

It can be shown from (A15) and (A16) that this is equivalent to expression (12):

$$\mu^2_{r\nu} = \frac{\mu_\nu^2}{|C_\nu|} \quad .$$

APPENDIX 2

NOTATION

The inclusion of plasma dielectric effects in scattering calculations brings in many parameters and raises problems of notation. The following set of symbols has been used throughout the present paper.

$A = \underline{E}/\underline{e}$, normalizing coefficient for polarization vector $\underline{e}$

$\underline{B}$ - steady magnetic field in the plasma, always taken to be in the Z direction

$C = \frac{C_G}{k^2}$, C_G = Gaussian curvature of the wave vector surface

$\underline{E}$ - complex electric field

G - geometrical form factor

I - (subscript) incident wave

- specific intensity

P_I - incident power

P_S - scattered power

R - function defined in Appendix 1

S - (subscript) scattered wave

- curvature of refractive index surface

$S(\underline{k},\omega)$, $S'(\underline{k},f)$ - scattering spectral function

T - (superscript) Fourier transform

V - scattering volume

W - electromagnetic energy flux

a^2 - beam cross-sectional area

$\underline{e}$ - unnormalised polarization vector

f - frequency (Hz)

$\underline{j}$ - current density

$\underline{k}$ - wave vector

$\hat{\underline{k}}$ - unit vector along $\underline{k}$

$\hat{\underline{p}}$ - unit vector normal to $\underline{k}$ in (x,z) plane

$\hat{\underline{r}}$ - unit vector along ray direction

r_o - classical electron radius = 2.8179×10^{-15} m

$\underline{v}_g$ - group velocity

$\underline{v}$ - electron velocity

$d^2\sum/(d\,\Omega_{kS}\cdot d\omega_S)$ - differential scattering cross-section per unit wave vector solid angle and angular frequency bandwidth

Ω - solid angle

Ω_k - wave vector solid angle

Ω_r - ray solid angle

$\alpha = \omega_{pe}^2/\omega^2$

$\beta = \omega_{ce}^2/\omega^2$

$\gamma = (\beta \sin^2\phi)^2 + 4\beta\,(1-\alpha)^2 \cos^2\phi$

$\delta = \phi - \rho$ = angle between wave vector and ray direction

ϵ_0 - permittivity of free space

$\underline{\underline{\epsilon}}$ - dielectric tensor, with components ϵ_1, ϵ_2, ϵ_3

θ - Thomson scattering angle between $\underline{k}_I$ and $\underline{k}_S$

θ_r - angle between $\hat{\underline{r}}_I$ and $\hat{\underline{r}}_S$

λ - polarization: +1 for O wave
-1 for X wave

- (subscript) polarization

- wavelength

μ - refractive index

μ_r - ray refractive index

ν - polarization (also subscript)

ξ - function defined in Appendix 1

ρ - angle between ray direction and $\underline{b}$

$\underline{\underline{\sigma}}$ - conductivity tensor

$d^2\sigma/(d\Omega_{rS}\cdot d\omega_S)$ - differential scattering cross-section per unit ray solid angle and angular frequency bandwidth

τ - time interval

ϕ - angle between wave vector and $\underline{B}$

χ - angle between ($\underline{k}_I$, $\underline{B}$) and ($\underline{k}_S$, $\underline{B}$) planes

ψ - angle of rotation about z axis

ω - angular frequency

ω_{pe} - electron plasma frequency

ω_{ce} - electron gyrofrequency

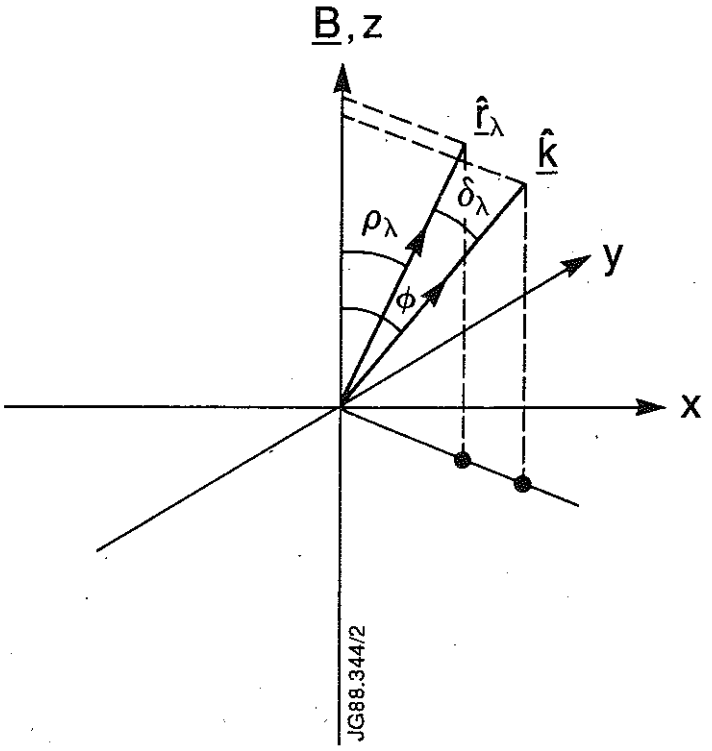

Fig. 1 Wave vector and ray directions. The magnetic field $\underline{B}$, the wave vector $\underline{k}$ and the ray direction $\hat{\underline{r}}_\lambda$ for polarization λ are in the same plane. $\delta_\lambda = \phi - \rho_\lambda$ is the angle between $\underline{k}$ and $\underline{r}_\lambda$.

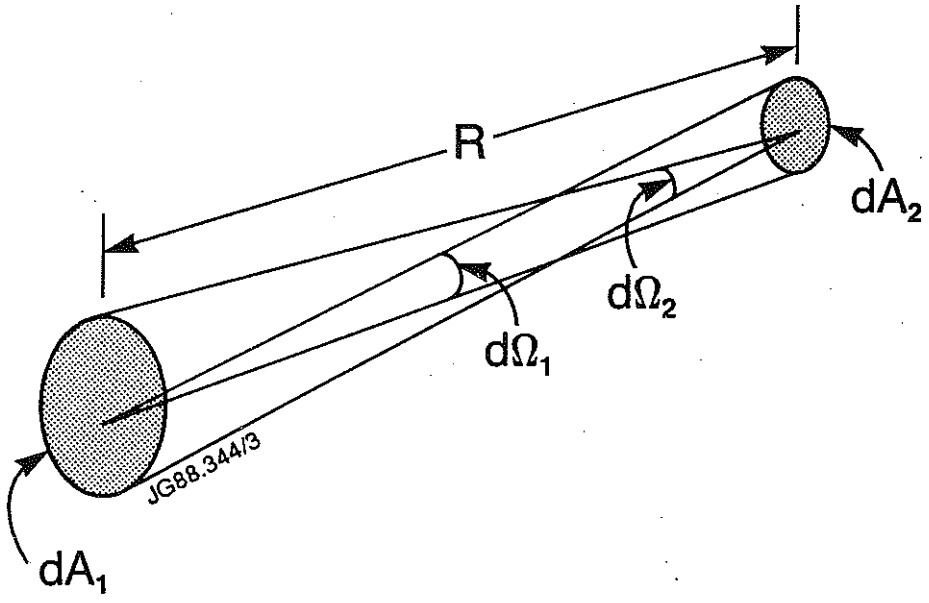

Fig. 2 Pencil of radiation in a loss-free, homogeneous, isotropic medium.

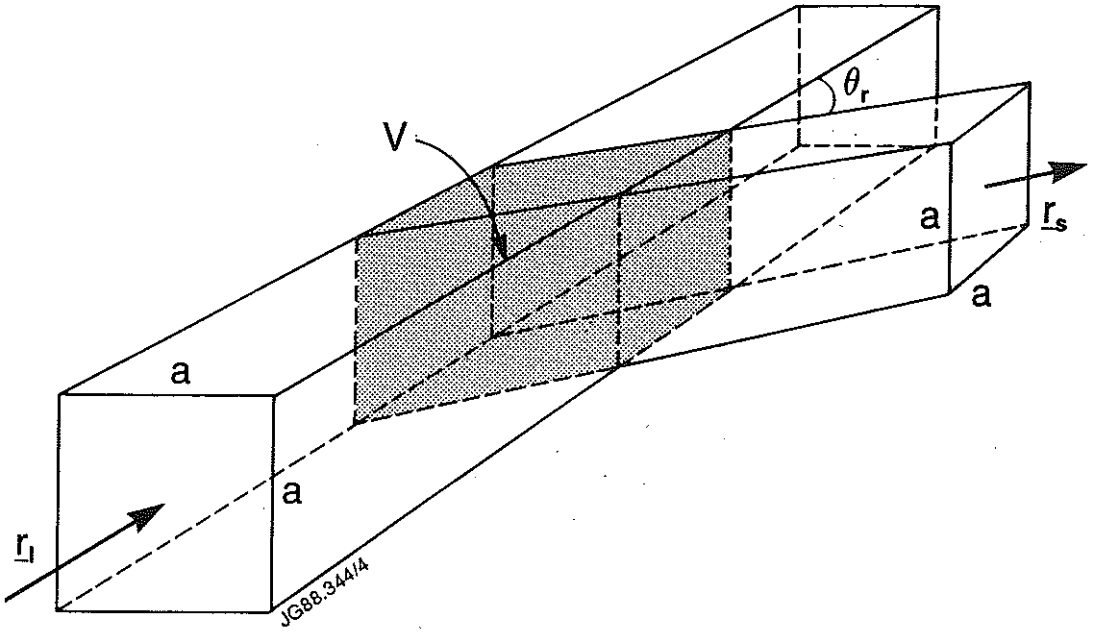

Fig.3 Simplified scattering geometry. The incident and scattered beams both have the same square cross-section with side a. The angle between their ray directions is θ_r.

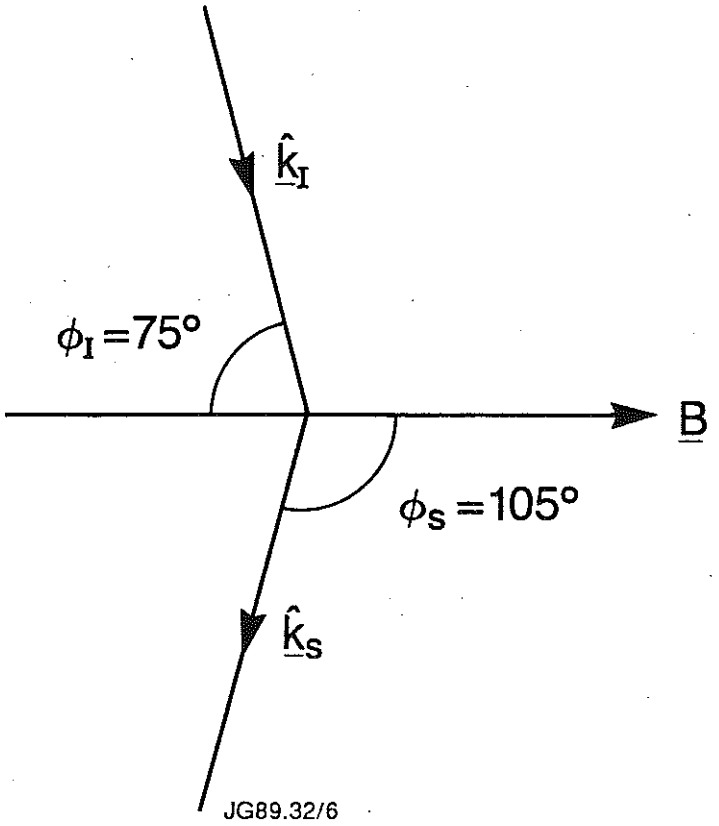

Fig.4 Scattering geometry used for numerical calculations of $G_{\lambda\nu}$.

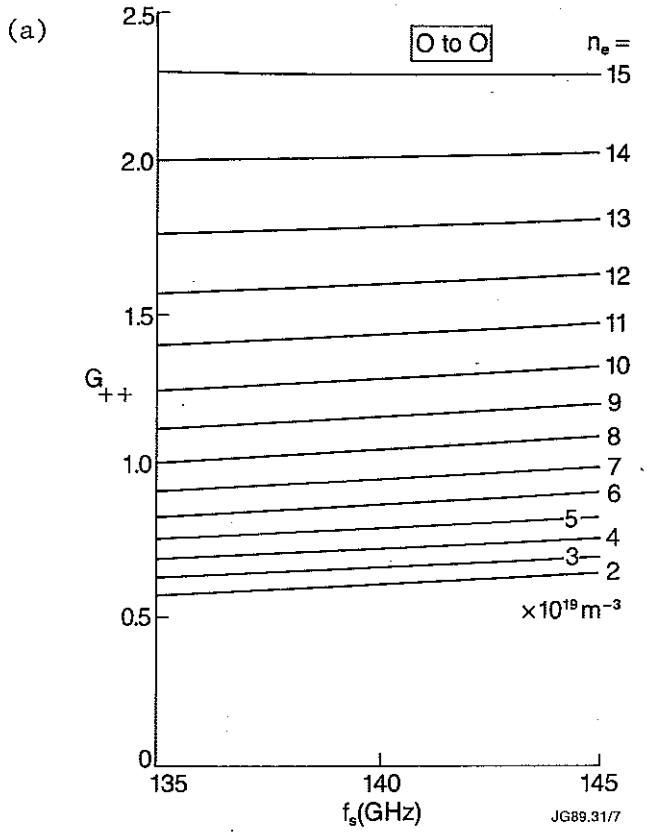

Fig. 5 Values of $G_{\lambda\nu}$ for scattering geometry of figure 4, in the electron density range 2×10^{19} to 1.5×10^{20} m^{-3}, for incident frequency 140 GHz, scattered frequencies in the range 135 to 145 GHz, with $B=3.4$ Tesla.

(a) O to O scattering
(b), (c) O to X scattering
(d), (e) X to O scattering
(f), (g) X to X scattering.

(b)

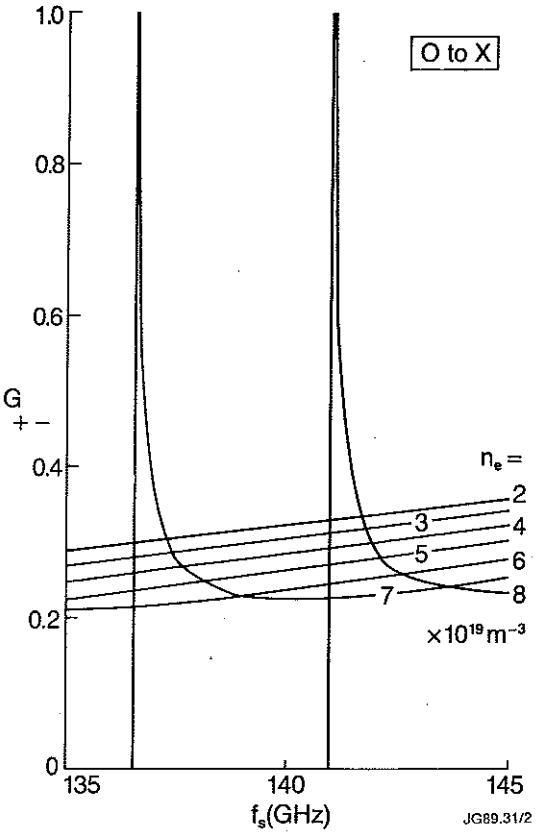
O to X
1.0
0.8
0.6
0.4
0.2
0
G
+ −
n_e =
2
3
4
5
6
7
8
×10¹⁹m⁻³
135
140
145
f_s(GHz)
JG89.31/2

(c)

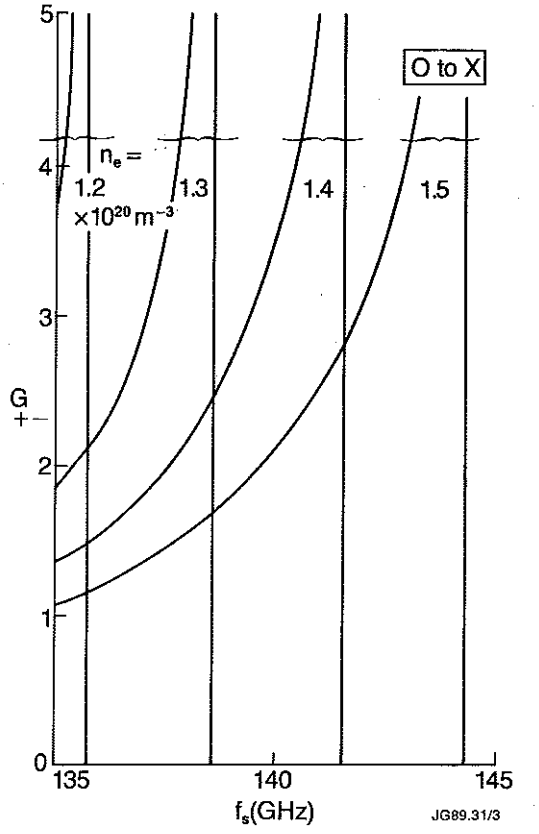
O to X
5
4
3
2
1
0
G
+ −
n_e =
1.2
×10²⁰m⁻³
1.3
1.4
1.5
135
140
145
f_s(GHz)
JG89.31/3

(d)

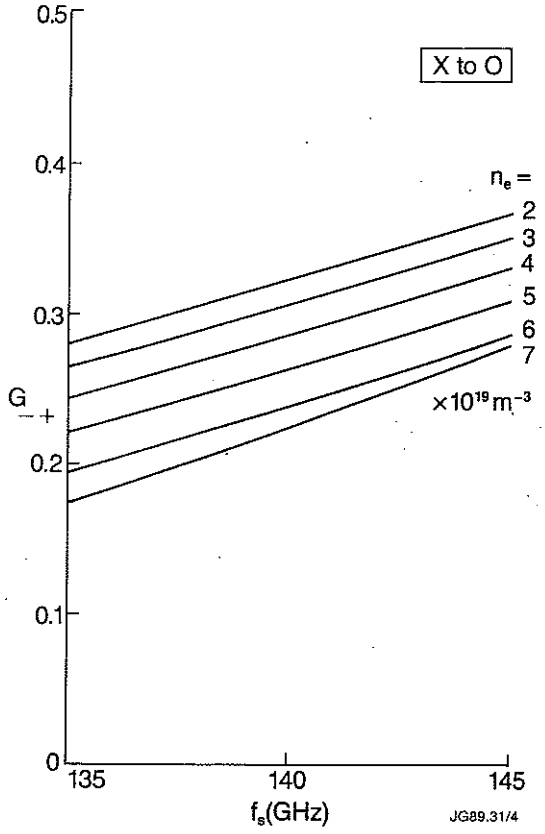
X to O
n_e =
2
3
4
5
6
7
$\times 10^{19} m^{-3}$
G
0.5
0.4
0.3
0.2
0.1
0
135
140
145
f_s(GHz)
JG89.31/4

(e)

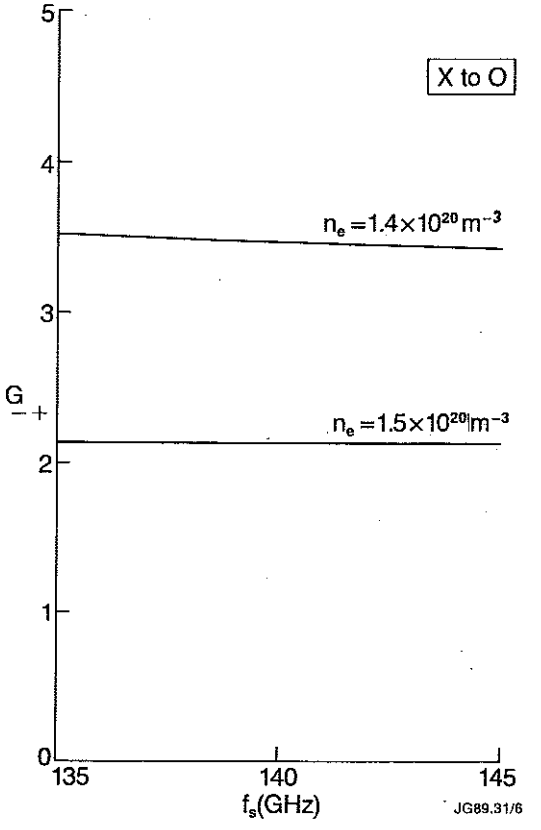
X to O
$n_e = 1.4 \times 10^{20} m^{-3}$
$n_e = 1.5 \times 10^{20} m^{-3}$
G
5
4
3
2
1
0
135
140
145
f_s(GHz)
JG89.31/6

(f)

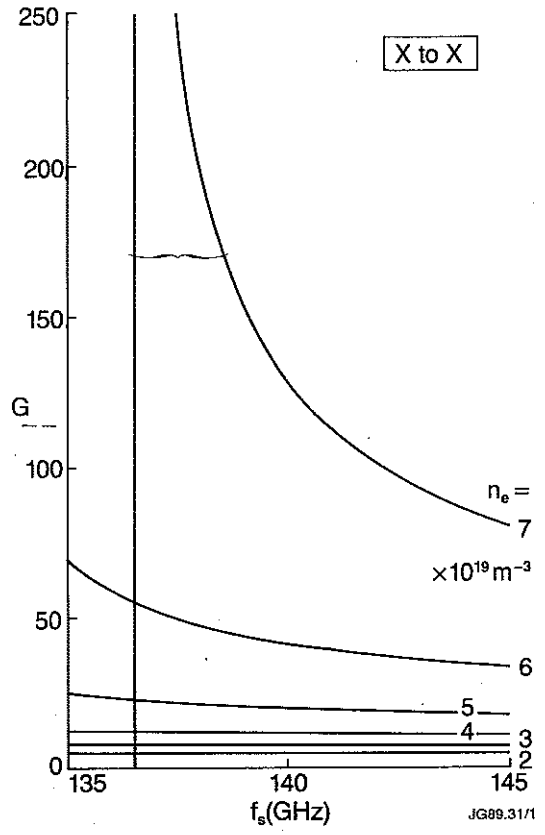
X to X
250
200
150
G
100
50
0
135
140
145
f_s(GHz)
n_e =
7
$\times 10^{19}$ m^{-3}
6
5
4
3
2
JG89.31/1

(g)

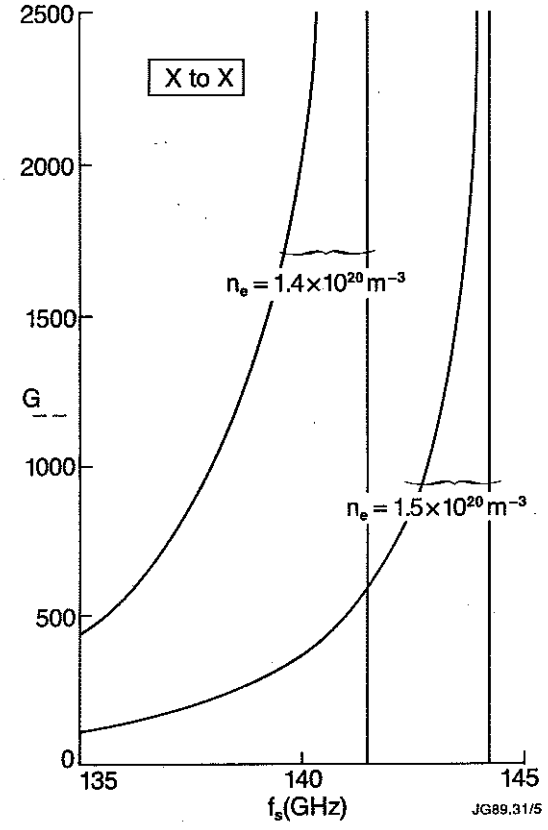
X to X
2500
2000
1500
G
1000
500
0
135
140
145
f_s(GHz)
$n_e = 1.4\times10^{20}$ m^{-3}
$n_e = 1.5\times10^{20}$ m^{-3}
JG89.31/5

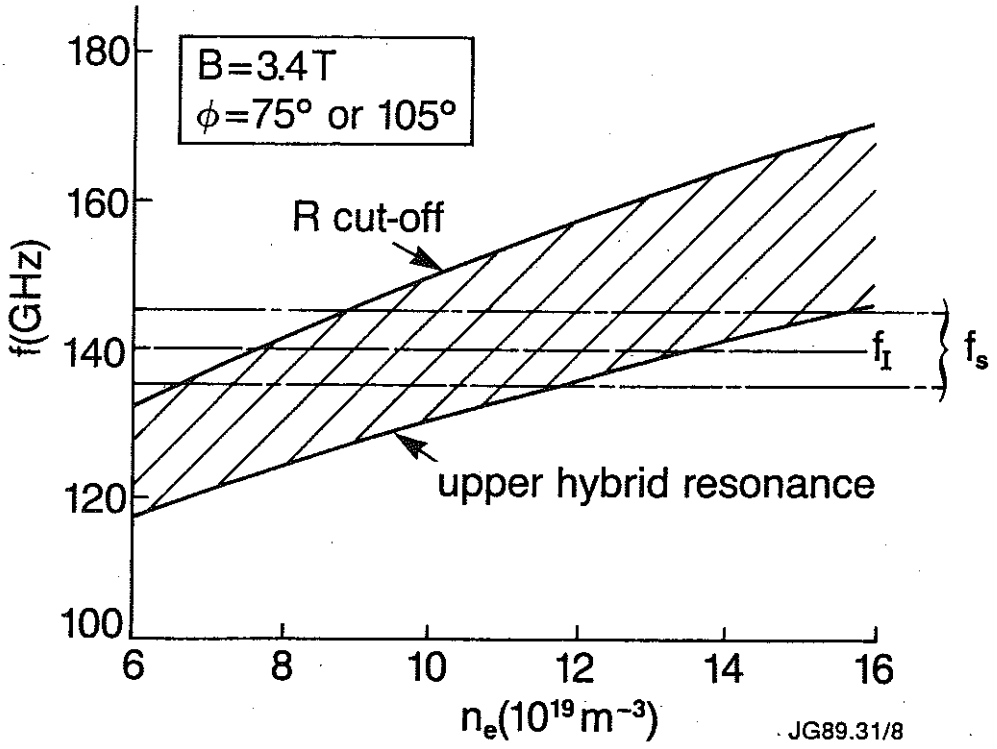

Fig. 6 Upper hybrid (ϕ=75° or 105°) and R cut-off frequencies for B=3.4T as functions of electron density.

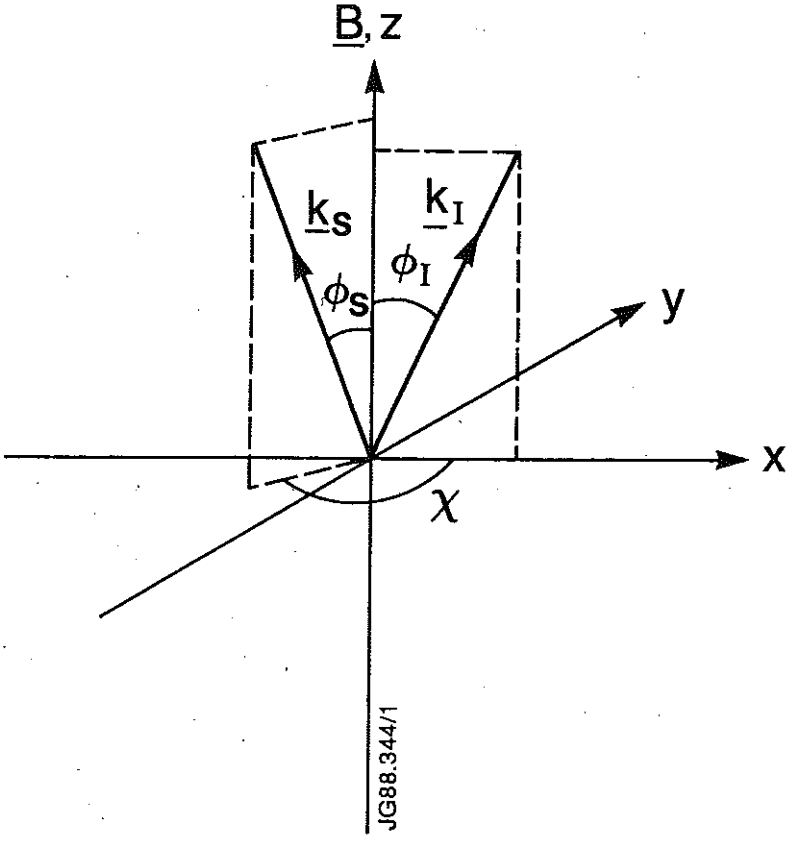

Fig. 7 General scattering geometry.
B is along z, k_I is in the (x, z) plane, ϕ_I is the angle between k_I and B, ϕ_S is the angle between k_S and B, and χ is the angle between the (k_I, B) and (k_S, B) planes.

APPENDIX 1.

THE JET TEAM

JET Joint Undertaking, Abingdon, Oxon, OX14 3EA, U.K.

J.M.Adams[1], F.Alladio[4], H.Altmann, R.J.Anderson, G.Appruzzese, W.Bailey, B.Balet, D.V.Bartlett, L.R.Baylor[24], K.Behringer, A.C.Bell, P.Bertoldi, E.Bertolini, V.Bhatnagar, R.J.Bickerton, A.Boileau[3], T.Bonicelli, S.J.Booth, G.Bosia, M.Botman, D.Boyd[31], H.Brelen, H.Brinkschulte, M.Brusati, T.Budd, M.Bures, T.Businaro[4], H.Buttgereit, D.Cacaut, C.Caldwell-Nichols, D.J.Campbell, P.Card, J.Carwardine, G.Celentano, P.Chabert[27], C.D.Challis, A.Cheetham, J.Christiansen, C.Christodoulopoulos, P.Chuilon, R.Claesen, S.Clement[30], J.P.Coad, P.Colestock[6], S.Conroy[13], M.Cooke, S.Cooper, J.G.Cordey, W.Core, S.Corti, A.E.Costley, G.Cottrell, M.Cox[7], P.Cripwell[13], F.Crisanti[4], D.Cross, H.de Blank[16], J.de Haas[16], L.de Kock, E.Deksnis, G.B.Denne, G.Deschamps, G.Devillars, K.J.Dietz, J.Dobbing, S.E.Dorling, P.G.Doyle, D.F.Düchs, H.Duquenoy, A.Edwards, J.Ehrenberg[14], T.Elevant[12], W.Engelhardt, S.K.Erents[7], L.G.Eriksonn[5], M.Evrard[2], H.Falter, D.Flory, M.Forrest[7], C.Froger, K.Fullard, M.Gadeberg[11], A.Galetsas, R.Galvao[8], A.Gibson, R.D.Gill, A.Gondhalekar, C.Gordon, G.Gorini, C.Gormezano, N.A.Gottardi, C.Gowers, B.J.Green, F.S.Griph, M.Gryzinski[26], R.Haange, G.Hammett[6], W.Han[9], C.J.Hancock, P.J.Harbour, N.C.Hawkes[7], P.Haynes[7], T.Hellsten, J.L.Hemmerich, R.Hemsworth, R.F.Herzog, K.Hirsch[14], J.Hoekzema, W.A.Houlberg[24], J.How, M.Huart, A.Hubbard, T.P.Hughes[32], M.Hugon, M.Huguet, J.Jacquinot, O.N.Jarvis, T.C.Jernigan[24], E.Joffrin, E.M.Jones, L.P.D.F.Jones, T.T.C.Jones, J.Källne, A.Kaye, B.E.Keen, M.Keilhacker, G.J.Kelly, A.Khare[15], S.Knowlton, A.Konstantellos, M.Kovanen[21], P.Kupschus, P.Lallia, J.R.Last, L.Lauro-Taroni, M.Laux[33], K.Lawson[7], E.Lazzaro, M.Lennholm, X.Litaudon, P.Lomas, M.Lorentz-Gottardi[2], C.Lowry, G.Magyar, D.Maisonnier, M.Malacarne, V.Marchese, P.Massmann, L.McCarthy[28], G.McCracken[7], P.Mendonca, P.Meriguet, P.Micozzi[4], S.F.Mills, P.Millward, S.L.Milora[24], A.Moissonnier, P.L.Mondino, D.Moreau[17], P.Morgan, H.Morsi[14], G.Murphy, M.F.Nave, M.Newman, L.Nickesson, P.Nielsen, P.Noll, W.Obert, D.O'Brien, J.O'Rourke, M.G.Pacco-Düchs, M.Pain, S.Papastergiou, D.Pasini[20], M.Paume[27], N.Peacock[7], D.Pearson[13], F.Pegoraro, M.Pick, S.Pitcher[7], J.Plancoulaine, J-P.Poffé, F.Porcelli, R.Prentice, T.Raimondi, J.Ramette[17], J.M.Rax[27], C.Raymond, P-H.Rebut, J.Removille, F.Rimini, D.Robinson[7], A.Rolfe, R.T.Ross, L.Rossi, G.Rupprecht[14], R.Rushton, P.Rutter, H.C.Sack, G.Sadler, N.Salmon[13], H.Salzmann[14], A.Santagiustina, D.Schissel[25], P.H.Schild, M.Schmid, G.Schmidt[6], R.L.Shaw, A.Sibley, R.Simonini, J.Sips[16], P.Smeulders, J.Snipes, S.Sommers, L.Sonnerup, K.Sonnenberg, M.Stamp, P.Stangeby[19], D.Start, C.A.Steed, D.Stork, P.E.Stott, T.E.Stringer, D.Stubberfield, T.Sugie[18], D.Summers, H.Summers[20], J.Taboda-Duarte[22], J.Tagle[30], H.Tamnen, A.Tanga, A.Taroni, C.Tebaldi[23], A.Tesini, P.R.Thomas, E.Thompson, K.Thomsen[11], P.Trevalion, M.Tschudin, B.Tubbing, K.Uchino[29], E.Usselmann, H.van der Beken, M.von Hellermann, T.Wade, C.Walker, B.A.Wallander, M.Walravens, K.Walter, D.Ward, M.L.Watkins, J.Wesson, D.H.Wheeler, J.Wilks, U.Willen[12], D.Wilson, T.Winkel, C.Woodward, M.Wykes, I.D.Young, L.Zannelli, M.Zarnstorff[6], D.Zasche[14], J.W.Zwart.

PERMANENT ADDRESS

1. UKAEA, Harwell, Oxon. UK.
2. EUR-EB Association, LPP-ERM/KMS, B-1040 Brussels, Belgium.
3. Institute National des Récherches Scientifique, Quebec, Canada.
4. ENEA-CENTRO Di Frascati, I-00044 Frascati, Roma, Italy.
5. Chalmers University of Technology, Göteborg, Sweden.
6. Princeton Plasma Physics Laboratory, New Jersey, USA.
7. UKAEA Culham Laboratory, Abingdon, Oxon. UK.
8. Plasma Physics Laboratory, Space Research Institute, Sao José dos Campos, Brazil.
9. Institute of Mathematics, University of Oxford, UK.
10. CRPP/EPFL, 21 Avenue des Bains, CH-1007 Lausanne, Switzerland.
11. Risø National Laboratory, DK-4000 Roskilde, Denmark.
12. Swedish Energy Research Commission, S-10072 Stockholm, Sweden.
13. Imperial College of Science and Technology, University of London, UK.
14. Max Planck Institut für Plasmaphysik, D-8046 Garching bei München, FRG.
15. Institute for Plasma Research, Gandhinagar Bhat Gujat, India.
16. FOM Instituut voor Plasmafysica, 3430 Be Nieuwegein, The Netherlands.
17. Commissiariat à L'Energie Atomique, F-92260 Fontenay-aux-Roses, France.
18. JAERI, Tokai Research Establishment, Tokai-Mura, Naka-Gun, Japan.
19. Institute for Aerospace Studies, University of Toronto, Downsview, Ontario, Canada.
20. University of Strathclyde, Glasgow, G4 ONG, U.K.
21. Nuclear Engineering Laboratory, Lapeenranta University, Finland.
22. JNICT, Lisboa, Portugal.
23. Department of Mathematics, Univeristy of Bologna, Italy.
24. Oak Ridge National Laboratory, Oak Ridge, Tenn., USA.
25. G.A. Technologies, San Diego, California, USA.
26. Institute for Nuclear Studies, Swierk, Poland.
27. Commissiariat à l'Energie Atomique, Cadarache, France.
28. School of Physical Sciences, Flinders University of South Australia, South Australia SO42.
29. Kyushi University, Kasagu Fukuoka, Japan.
30. Centro de Investigaciones Energeticas Medioambientales y Techalogicas, Spain.
31. University of Maryland, College Park, Maryland, USA.
32. University of Essex, Colchester, UK.
33. Akademie de Wissenschaften, Berlin, DDR.

CR 88.49.1A